الجمهورية الجزائرية الديمقراطية الشعبية
وزارة التعليم العالي و البحث العلمي

People's Democratic Republic of Algeria
Ministry of Higher Education and Scientific Research

University of RELIZANE
Faculty of Science and Technology
Department: Chemistry

جامعة غليزان
RELIZANE UNIVERSITY

THESIS

In order to obtain the MASTER degree in :

Chemistry of materials

Title

Synthesis of composites for catalytic reactions

Presented by:

Miss :

DJERIOU Nour El Houda

In the presence of jury members:

Chairman: Dr	BOUCHERDOUD Ahmed	Senior lecturer (A) at (U. Relizane)
Supervisor: Dr	HACHEMAOUI Mohammed	Senior lecturer (B) at (U. Relizane)
Reviewer: Dr	BENDJELLOUL Meriem	Senior lecturer (A) at (U. Relizane)

Academic year: 2023/2024

Acknowledgments

In the name of Allah, the Most Gracious, the Most Merciful. All praise is due to Allah, who has granted me the strength, patience, and wisdom to complete this work. Without His guidance and blessings, this achievement would not have been possible.

I would like to express my deepest gratitude to my supervisor, Dr. HACHEMAOUI Mohammed, for his invaluable guidance, support, and encouragement throughout the course of this research. His expertise and insights have been instrumental in the successful completion of this thesis.

I am also profoundly grateful to the Materials Chemistry Laboratory at the University of Relizane for providing the necessary resources and a conducive environment for my research. Additionally, I extend my heartfelt thanks to the Laboratory of Chemistry at University (Oran 1) for their support and collaboration.

I would like to acknowledge the members of my jury, BOUCHERDOUD Ahmad and BENDJELLOUL Meriem, for their time, effort, and valuable feedback, which have greatly contributed to the improvement of this work.

My sincere thanks go to all the professors who have taught me throughout my university career at Relizane University. Their knowledge and dedication have been a source of inspiration and have significantly shaped my academic journey.

Finally, I am deeply thankful to all my friends and colleagues, as well as everyone who has encouraged and supported me directly or indirectly during the completion of this work. Your unwavering support and encouragement have been a constant source of motivation

Dedication

To my beloved parents,

My mother and my father, your endless sacrifices, boundless love, and unwavering support have been the foundation of my success. Your prayers, encouragement, and belief in me have been my guiding light throughout my academic journey. May God protect you and grant you happiness, and may success always be within my reach so that I can continue to fill your hearts with joy.

To my dear sisters,

Fatima Zohra, Zoulikha, Sarah, Wassila and Safia, your constant encouragement and moral support have been my strength. Thank you for always being there and for believing in me.

To Mr. Hachemaoui Mohammed,

Your guidance and insightful advice have been invaluable. I am deeply grateful for your support, valuable suggestions, and tireless efforts.

To all my classmates

Thank you for the wonderful years we spent together during our university studies. Your companionship and shared experiences have made this journey memorable.

And last but not least, to all my friends, especially my best friend and sister, Goufa Nora,

Thank you for your friendship and support. you have made this journey enjoyable and unforgettable

Nour el Houda

Abstract:

Water pollution poses a significant threat to ecosystems and human health, driven by industrial waste and agricultural runoff containing harmful dyes and phenolic compounds. This research aims to synthesize and evaluate novel composites of graphitic carbon nitride (g-C3N4) modified with silver nanoparticles for their catalytic properties in degrading these pollutants. The methodology involved synthesizing g-C3N4 via thermal polymerization of melamine, followed by modification with silver nanoparticles through a reduction process. The composites were characterized using X-ray diffraction (XRD), scanning electron microscopy (SEM), and Fourier-transform infrared spectroscopy (FTIR). Catalytic performance was assessed through the degradation of methylene blue and phenol under visible light irradiation. The results indicated that silver-modified g-C3N4 exhibited superior catalytic activity compared to unmodified g-C3N4, achieving over 90% degradation efficiency for both pollutants. These findings underscore the potential of these composites for environmental remediation applications.

الملخص :

يشكل تلوث المياه تهديدًا كبيرًا للنظم البيئية وصحة الإنسان، مدفوعًا بالنفايات الصناعية والجريان السطحي الزراعي الذي يحتوي على أصباغ ضارة ومركبات فينولية. تهدف هذه الدراسة إلى تخليق وتقييم مركبات جديدة من نيتريد الكربون الجرافيتي (g-C3N4) المعدلة بجسيمات الفضة النانوية لخصائصها التحفيزية في تحلل هذه الملوثات. تضمنت المنهجية تخليق عبر البلمرة الحرارية للميلامين، ثم التعديل بجسيمات الفضة النانوية من خلال عملية اختزال. تم توصيف المركبات باستخدام حيود الأشعة السينية (XRD) والمجهر الإلكتروني الماسح (SEM) ومطياف الأشعة تحت الحمراء (FTIR), تم تقييم الأداء التحفيزي من خلال تحلل الميثيلين الأزرق والفينول تحت إشعاع الضوء المرئي. أشارت النتائج إلى ان محفز g-C3N4 المعدل بالفضة أظهر نشاطًا تحفيزيًا فائقًا مقارنةً بـ g-C3N4 غير المعدل، حيث حقق كفاءة تحلل تزيد عن 90% لكلا الملوثين. تؤكد هذه النتائج على إمكانات هذه المركبات في تطبيقات معالجة التلوث البيئي.

Résumé :

La pollution de l'eau constitue une menace significative pour les écosystèmes et la santé humaine, alimentée par les déchets industriels et les ruissellements agricoles contenant des colorants nocifs et des composés phénoliques. Cette recherche vise à synthétiser et évaluer de nouveaux composites de nitrure de carbone graphitique (g-C3N4) modifiés avec des nanoparticules d'argent pour leurs propriétés catalytiques dans la dégradation de ces polluants. La méthodologie comprenait la synthèse du g-C3N4 par polymérisation thermique de la mélamine, suivie d'une modification avec des nanoparticules d'argent par un processus de réduction. Les composites ont été caractérisés à l'aide de la diffraction des rayons X (XRD), de la microscopie électronique à balayage (SEM) et de la spectroscopie infrarouge à transformée de Fourier (FTIR). La performance catalytique a été évaluée par la dégradation du bleu de méthylène et du phénol sous irradiation de lumière visible. Les résultats ont indiqué que le g-C3N4 modifié avec de l'argent présentait une activité catalytique supérieure par rapport au g-C3N4 non modifié, atteignant une efficacité de dégradation de plus de 90 % pour les deux polluants. Ces résultats soulignent le potentiel de ces composites pour les applications de réhabilitation environnementale.

LIST OF ABBREVIATIONS

List of abbreviations

g-C_3N_4	Graphitic Carbon Nitride
MO	Methyl Orange
MB	Methylene Blue
$NaBH_4$	Sodium Borohydride
Ag	Silver
FTIR	Fourier Transform Infrared Spectroscopy
UV-Vis	Ultraviolet-Visible Spectroscopy
IUPAC	International Union of Pure and Applied Chemistry
AgNPs	Silver Nanoparticles
XRD	X-ray Diffraction
MOFs	Metal-Organic Frameworks
PTFE	Poly tetrafluoro ethylene
PMCs	Polymer Matrix Composites
MMCs	Metal Matrix Composites
CMCs	Ceramic Matrix Composites
CMNC	Ceramic Matrix Nanocomposites
MMNC	Metal Matrix Nanocomposites
PMNC	Polymer Matrix Nanocomposites
SPR	Surface Plasmon Resonance

LIST OF ILLUSTRATIONS

List of Figures

Bibliographic Study

Methods And Martials

List of Tables

Bibliographic Study

Methods and materials

Contents

GENERAL INTRODUCTION

in recent years, the rapid pace of industrialization has significantly escalated environmental challenges, particularly in the realms of air, soil, and water pollution. Among these, water pollution is of utmost concern due to its profound impact on all living organisms[1]. Despite the Earth's surface being predominantly covered by water, only a minuscule fraction, about 0.5%, is accessible and suitable for human consumption and agricultural activities. This precious resource is increasingly threatened by contamination from various pollutants, posing severe risks to health and ecosystems[2].

Industrial processes discharge a vast array of toxic substances, notably dyes and phenolic compounds, into the environment. These pollutants are notorious for their chemical stability, making them resistant to natural degradation and persistent in ecosystems. The dyeing industry alone is a major contributor, annually releasing significant quantities of dyes that pollute water bodies and disrupt aquatic life[3].

To combat these issues, a variety of advanced wastewater treatment technologies have been developed. Techniques such as membrane bioreactors, photocatalysis, advanced oxidation processes, electrochemical treatments, UV disinfection, and the use of metal nanoparticles have shown promise in reducing water pollutants. However, the quest for more efficient, cost-effective, and sustainable solutions continues to drive scientific and engineering innovation[4].

Addressing water pollution is critical for ensuring the sustainability of our water resources. Through the development and implementation of novel treatment methods, we can effectively reduce environmental pollutants and protect the vital water supply necessary for life on Earth like synthesis of composites for catalytic reactions based on nanoparticles for catalytic reactions[5]

the Graphitic carbon nitride (g-C_3N_4) has emerged as a promising material in the field of environmental remediation due to its unique properties. As a polymeric semiconductor, g-C_3N_4 is characterized by its high surface area, thermal stability, and chemical robustness. Its porous structure allows for significant interaction with pollutants, making it an excellent candidate for catalytic applications. The material's ability to act as a photocatalyst under visible light further enhances its utility in degrading organic pollutants in water. The modification of g-C_3N_4 with silver nanoparticles can enhance its catalytic efficiency by improving electron conductivity and photocatalytic activity, making it more effective in reducing pollutants such as dyes and phenolic compounds[6].

This thesis is structured into 3 chapters, each detailing a specific aspect of the research:

Chapter I the Bibliographic Study, this chapter provides a comprehensive overview of porous materials, polymers, and composites, with a particular focus on g-C_3N_4. It delves into the historical background, synthesis methods, and properties of g-C_3N_4, including its structural, chemical, and physical characteristics.

The chapter also discusses the modification of g-C3N4, particularly with silver nanoparticles, to enhance its catalytic properties. Additionally, it covers the types of dyes commonly found in industrial effluents and the various techniques used for the characterization of materials, such as X-ray diffraction (XRD), Fourier-transform infrared spectroscopy (FTIR), and UV-Vis spectrophotometry.

Chapter II the Experimental Study, this chapter outlines the materials and methods used in the synthesis and modification of g-C_3N_4. It details the experimental procedures for preparing g-C_3N_4 from melamine, modifying it with silver nitrate, and reducing it with sodium borohydride to form silver-modified g-C_3N_4 composites.

The chapter includes step-by-step descriptions of the synthesis processes, observations, and the conditions under which the experiments were conducted.

Chapter III the Results and Application, this chapter presents the results of the experimental studies, including the characterization of the synthesized materials. It discusses the XRD and FTIR spectra of the g-C_3N_4 and Ag@g-C_3N_4 nanocomposites, highlighting the structural and chemical changes resulting from the modification. The chapter also explores the application of these materials in catalytic reduction reactions, specifically focusing on the reduction of dyes such as methylene blue and methyl orange. The efficiency of the catalysts is evaluated under various conditions, and the factors influencing the reduction process are analyzed.

Through this work, we aim to contribute to the development of more effective and sustainable solutions for water pollution, leveraging the unique properties of g-C_3N_4 and its composites**.**

BIBLIOGRAPHIC STUDY

I.1. Introduction

Chapter I provides an extensive overview of the fundamental concepts and materials relevant to this research. We begin by exploring the properties and classifications of porous materials, which are critical for various applications, including catalysis. This chapter delves into the unique characteristics of graphitic carbon nitride (g-C_3N_4), a promising material for environmental remediation due to its high surface area, thermal stability, and photocatalytic properties. We also discuss the synthesis methods and modifications of g-C_3N_4, particularly its enhancement with silver nanoparticles to improve catalytic efficiency. Additionally, the chapter covers the types of dyes commonly found in industrial effluents and the various techniques used for the characterization of materials, such as X-ray diffraction (XRD), Fourier-transform infrared spectroscopy (FTIR), and UV-Vis spectrophotometry. This comprehensive bibliographic study sets the stage for the experimental investigations and applications discussed in subsequent chapters.

I.2.Porous Materials

Porous materials are solids characterized by a solid matrix and a void phase, where the voids are accessible and permeable to fluids (liquids or gases).[7] These voids, also known as pores, can be cavities, channels, or interstices, which are typically deeper than they are wide. The porosity of these materials allows for various interactions with gases and liquids, depending on the size, shape, and connectivity of the pores [8]

The International Union of Pure and Applied Chemistry (IUPAC) classifies porous materials based on the size of their pores into three categories: microporous, mesoporous, and macroporous materials[9]

Table 01: IUPC Classification of Porous Materials

Pore Size Category	Pore Diameter
Microporous	< 2nm
Mesoporous	2nm≤ d ≤50nm
Macroporous	> 50nm

Porous materials can also be divided into two categories based on their origin[10]:

- **Natural Porous Materials:** This category includes materials like rocks, zeolites, and wood, which occur naturally. Natural porous materials are often used in environmental applications, such as water filtration and soil conditioning.[11]
- **Synthetic Porous Materials**: These are engineered to meet specific industrial and technological needs. Examples include polymer foams and synthetic zeolites, which are used in a wide range of applications from insulation and shock protection to catalysis and construction materials. The synthesis of these materials often involves complex methods designed to achieve particular properties.[10]

the unique properties of porous materials, such as high surface area, tailored porosity and pore size distribution, and exceptional thermal and chemical stability, porous materials with her properties also offer versatile applications in energy conversion, environmental protection, and chemical synthesis.[12]

Porous materials are distinguished by their unique structural features, primarily characterized by the presence of voids or pores within their solid matrix.[7]

This distinctive architecture endows them with a variety of properties that are highly valued across numerous scientific and technological fields, particularly in catalysis.[13]

These materials encompass a broad spectrum of substances, including zeolites, metal-organic frameworks (MOFs), and carbon-based materials such as activated carbon and graphitic carbon nitride (g-C_3N_4).[14]

High Surface Area

A pivotal property of porous materials is their high surface area, which significantly enhances their utility in catalytic applications.[15] The extensive surface area provides numerous active sites for catalytic reactions, facilitating efficient interactions with reactants. This characteristic is especially advantageous in adsorption processes, where the material's capacity to adsorb and retain substances is crucial.[12] For instance, zeolites, known for their microporous structure, are highly effective in refining processes, such as cracking heavy petroleum fractions into lighter, more valuable fractions.[16]

Porosity and Pore Size Distribution

The porosity and the specific distribution of pore sizes within porous materials critically influence their effectiveness in catalytic reactions.[12] These structural features affect the

diffusion rates of reactants and products to and from the active sites, thereby impacting the overall reaction efficiency [17] MOFs are exemplary in this regard, offering tunable pore sizes that can be precisely controlled to optimize reactant accessibility and catalytic activity. This makes MOFs ideal for a variety of chemical reactions, including the conversion of CO_2 into useful chemicals. [18]

Thermal Stability

Many catalytic processes operate under high temperatures, necessitating materials that can withstand such conditions without degrading.[19] Porous materials, particularly certain carbon-based types like g-C_3N_4, exhibit remarkable thermal stability.[20] This property makes them suitable for high-temperature catalytic applications, including photocatalytic reactions such as water splitting and pollutant degradation under visible light irradiation.[20] g-C_3N_4's stability under these conditions underscores its utility in sustainable energy and environmental remediation applications.

Chemical Stability

The chemical stability of porous materials is essential for maintaining their structural integrity and functionality in various chemical environments. This stability enables their use in a wide range of catalytic and chemical processes.[19] For example, silica-based mesoporous materials are particularly valued in acid-catalyzed reactions due to their resistance to acidic conditions, facilitating their application in the synthesis of fine chemicals and other specialized chemical processes[21].

I.2. Polymer Materials

The term "polymer" is derived from two Greek words: 'poly,' meaning 'many,' and 'mer,' meaning 'part.' A polymer is a macromolecule, either organic or inorganic, with a very high molar mass, formed by the covalent bonding of a large number of repeating units derived from one or more types of monomers. Polymers are synthesized through a process known as polymerization, where monomers are connected by strong covalent bonds to form lengthy chains.[22]

Polymers can be categorized as natural, such as DNA and proteins, or synthetic, like plastics and nylon[23]. Additionally, there are semi-synthetic polymers, which are derived from natural polymers but chemically modified to enhance their properties, an example being cellulose acetate.[24]

Polymers are versatile materials whose properties can be engineered to meet the demands of various applications, including catalysis, where their physical and chemical stability, along with the ability to incorporate functional catalytic groups[25]

Polymers exhibit a range of physical properties that can be manipulated based on their molecular structure and processing. These properties include tensile strength, elasticity, and thermal stability[22]. For instance, high-density polyethylene (HDPE) has a melting point of around 130°C and is known for its strength and rigidity, making it ideal for products like plastic bottles and piping [26]

Polymers are very resistant to acids, bases, and other solvents, making them suitable for containers and coatings. For example, Teflon (PTFE), known for its non-stick properties, has a very high resistance to chemical attack and can withstand temperatures up to 250°C without degrading [26]

Polymers are chosen in catalytic reactions for their ability to provide high surface areas and the possibility to functionalize their surface with catalytic sites.[27] Polystyrene-divinylbenzene copolymers are often used as supports for catalysts in organic synthesis due to their stability and ease of functionalization. These materials can be used to anchor metal catalysts or to create acidic or basic sites depending on the required reaction.[27]

Polymers like polyaniline and polypyrene are also used in catalytic contexts for their conductive properties, which can be crucial in electrocatalysis. The specific surface area and porosity of these polymers can be adjusted during synthesis, which is critical for their effectiveness in catalytic roles.[28]

I.3.Composites Materials

A composite material is a material made from two or more constituent materials with significantly different physical or chemical properties. These materials remain distinct within the finished structure, resulting in a material with properties that are different from the individual components. The primary components of a composite are the matrix (or binder) and the reinforcement. [29]

The matrix surrounds and supports the reinforcement materials by maintaining their relative positions, while the reinforcement imparts its special mechanical and physical properties to enhance the matrix properties[30].

- **Matrix**: The continuous phase that binds the reinforcement materials together. It can be made of polymers, metals, or ceramics[31].
- **Reinforcement**: The dispersed phase that provides strength and stiffness. It can be in the form of fibers, particles, or flakes and is typically made of materials like glass, carbon, or aramid fibers[32].

Composites are classified based on the matrix material and the reinforcement material used.:

1. Polymer Matrix Composites (PMCs): These composites use a polymer-based matrix and are reinforced with fibers like glass, carbon, or aramid. PMCs are known for their lightweight and corrosion-resistant properties[33]

2. Metal Matrix Composites (MMCs)[34]**:** MMCs have a metal matrix. Reinforcements in MMCs can include ceramics or carbon fibers, offering high strength and stiffness as well as thermal and electrical conductivity

3. Ceramic Matrix Composites (CMCs): In CMCs, the matrix is ceramic, reinforced with fibers like carbon or silicon carbide. These composites are used in high-temperature applications due to their ability to withstand extreme heat[35]

I.4.Nano-Composites Materials

Nanocomposites are a type of composite material where at least one of the phases has dimensions in the nanometer range (1 nm = 10^{-9} m). These materials are (heterogeneous/hybrid) materials produced by mixing polymers with inorganic solids (such as clays, oxides, or metals) at the nanoscale. The properties of nanocomposites are influenced by their structure, composition, interfacial interactions, and the properties of the individual components.[36] They are classified based on their matrix materials into three main types: ceramic matrix nanocomposites (CMNC), metal matrix nanocomposites (MMNC), and polymer matrix nanocomposites (PMNC)[37].

1. Ceramic Matrix Nanocomposites (CMNC): These nanocomposites incorporate ceramic materials as the matrix and are known for their high thermal stability and mechanical strength. They are used in high-temperature applications and structural components[38]

2. Metal Matrix Nanocomposites (MMNC): These nanocomposites use metals as the matrix and often include metal or ceramic nanoparticles. They provide enhanced electrical conductivity, thermal stability, and mechanical properties, making them suitable for aerospace, automotive, and electronic applications[37]

3. Polymer Matrix Nanocomposites (PMNC): These consist of a polymer matrix embedded with inorganic nanoparticles such as clays, metals, or oxides. They offer improved mechanical properties, thermal stability, and reduced permeability, making them ideal for applications in packaging, electronics, and biomedical fields[39]

Nanocomposites are chosen for catalytic applications due to several advantageous properties that significantly enhance their performance. One of the primary reasons is their enhanced surface area. Nanocomposites possess a high surface area, which provides more active sites for catalytic reactions, thereby increasing catalytic activity[40]. For instance, polymer nanocomposites with carbon nanotubes can exhibit surface areas as high as 1000 m^2/g, which is substantially higher than traditional catalysts.[41]

Nanocomposites exhibit high activity and stability, particularly those based on metals like silver[42]. Silver-based nanocomposites are known for their high catalytic activity and stability, making them efficient for various catalytic processes such as oxidation and reduction reactions. For example, Ag-based nanocomposites have been shown to maintain their catalytic activity over multiple cycles, demonstrating their stability and reusability [43]

The combination of different materials in nanocomposites can lead to synergistic effects that further improve catalytic performance. These effects can enhance charge transfer and reaction rates[44]. For instance, $MnCo_2O_4/NiCo_2O_4$/rGO nanocomposites facilitate electrochemical reactions by providing efficient charge transfer pathways, resulting in improved catalytic efficiency[45]. Similarly, ZrO_2/NiO/rGO composites have shown enhanced catalytic activity due to the synergistic interaction between the components [46]

Nanocomposites also offer tunable properties, allowing for the optimization of catalytic properties for specific reactions. By adjusting the type and amount of constituent materials, the properties of nanocomposites can be tailored to meet the requirements of particular catalytic processes. For example, the incorporation of different metal oxides into polymer matrices can be adjusted to optimize the catalytic activity for environmental remediation applications [47]

Nanocomposites can improve the selectivity and reducibility of catalysts, making them more effective for targeted reactions. For instance, (Ag)Pd-Fe_3O_4 nanocomposites have shown high selectivity to formaldehyde in methane partial oxidation at low temperatures. The incorporation of Ag into the Pd-Fe_3O_4 system enhances the reducibility of Fe_3^+ species, which is crucial for the catalytic process [48]

I.5.Historical background of graphitic carbon nitride (g-C_3N_4)

Graphitic carbon nitride (g-C_3N_4) is a material with a rich and evolving history that dates back to the early 19th century. The earliest known report of a carbon nitride compound can be attributed to the work of Berzelius and Liebig in 1834, who synthesized a material they named "melon" through the polymerization of cyanamide. This discovery marks the inception of carbon nitride research, situating its origin in the 19th century. However, it remained largely theoretical without any practical synthesis or application. This period was marked by theoretical chemists pondering the possibilities of new materials but lacking the means to create them[49].

The modern chapter in the story of g-C_3N_4 began with the theoretical predictions by Marvin Cohen and Amy Liu from the University of California, Berkeley, in the late 1980s. They hypothesized the existence of a superhard material based on a carbon nitride compound, which they suggested could be harder than diamond. This prediction rekindled interest in the carbon-nitride framework and set the stage for experimental efforts.[50]

The landmark experimental breakthrough came in 2009 when Markus Antonietti and Xinchen Wang, along with their team at the Max Planck Institute of Colloids and Interfaces in Germany, successfully synthesized g-C_3N_4. They used melamine as a precursor, employing a simple heating process to create a polymer that exhibited properties suitable for photocatalysis under visible light. This synthesis not only confirmed the material's existence but also demonstrated its potential applications, particularly in the field of sustainable energy[51]

Throughout its development, numerous scientists have contributed to the understanding and enhancement of g-C_3N_4. Notable among them are researchers like Richard B. Kaner from UCLA, who explored various derivatives and applications of the material[52]. Theoretical support from scientists like David Teter and Russell J. Hemley further solidified understanding of its structure and properties.[53]

In recent years, the focus has shifted towards enhancing the photocatalytic efficiency of g-C_3N_4. Techniques such as doping with metals and non-metals, creating heterojunctions, and modifying the nanostructure have been employed to improve its light absorption capabilities and charge carrier separation. These modifications have led to improved performance in various photocatalytic processes, pushing g-C_3N_4 to the forefront of research in photocatalysis and environmental remediation[54] [55]

Today, g-C_3N_4 is celebrated not just for its potential in environmental applications but also as a symbol of how theoretical science can lead to practical innovations. The journey from a theoretical concept to a cornerstone in sustainable material science is a compelling story of curiosity, innovation, and the enduring spirit of scientific exploration. Researchers continue to explore new ways to enhance its properties and expand its applications, ensuring that g-C_3N_4 remains a vital material in the quest for sustainable solutions[56]

I.6.Graphite carbon nitride g-C_3N_4

Graphitic carbon nitride (g-C_3N_4) is a two-dimensional (2D) polymeric material composed primarily of carbon and nitrogen atoms arranged in a graphitic-like structure[57]. Has a general formula of $(C_3N_3H)_n$ it is a family of carbon nitride compounds with a general formula close to C_3N_4, typically containing non-zero amounts of hydrogen[58].

It is characterized by its rich properties, basic surface functionalities, and hydrogen-bonding motifs due to the presence of nitrogen and hydrogen atoms. His unique properties make him the famous potential candidate to complement carbon in various material applications[59]

I.6.1 Structure of graphite carbon nitride g-C_3N_4

The Overall Structure of g-C_3N_4 is a two-dimensional, layered material composed of two primary building units: s-triazine and s-heptazine (tri-s-triazine)[57].These s-triazine or s-heptazine units linked together through planar, sp2-hybridized carbon-nitrogen bonds. The layers are held together by van der Waals forces[60]. And the Arrangement of the structure is the s-triazine or s-heptazine units form a repeating pattern, creating a stable, planar network. The structure can be visualized as a series of interconnected hexagonal rings, similar to the structure of graphite but with nitrogen atoms incorporated into the rings.[61]

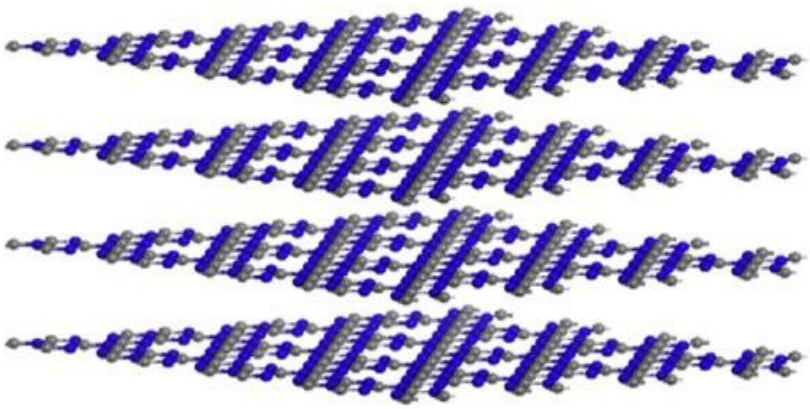

Figure 01: Molecular structure re of graphitic carbon nitride

- **s-Triazine Unit**

The Structure s-Triazine is a six-membered ring containing three carbon atoms and three nitrogen atoms arranged alternately. Each nitrogen atom is bonded to a hydrogen atom (NH_2 group) and its Chemical Formula is ($C_3N_3H_3$)[62]

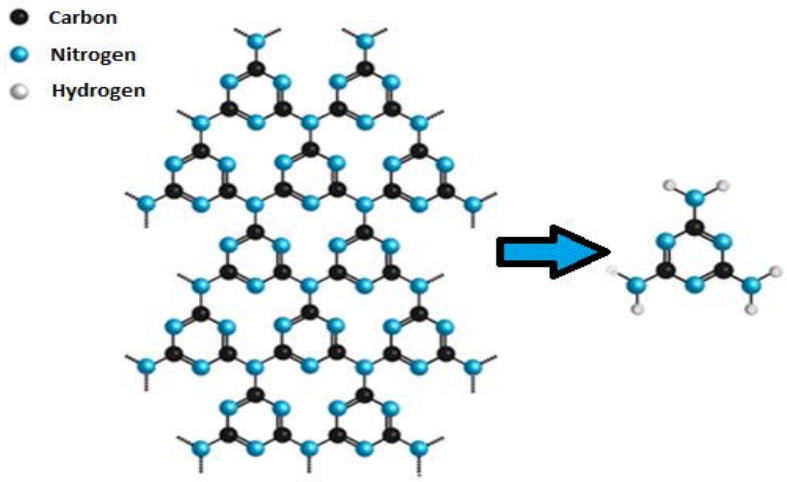

Figure 02: Molecular Structure of s-Triazine unit

- **s-Heptazine Unit**

The Structure s-Heptazine (tri-s-triazine) consists of three fused s-triazine rings, forming a larger, more complex structure. It has a central six-membered ring with three nitrogen atoms and three carbon atoms, each connected to an additional s-triazine ring. And its Chemical Formula is $C_6N_7H_3$[62]

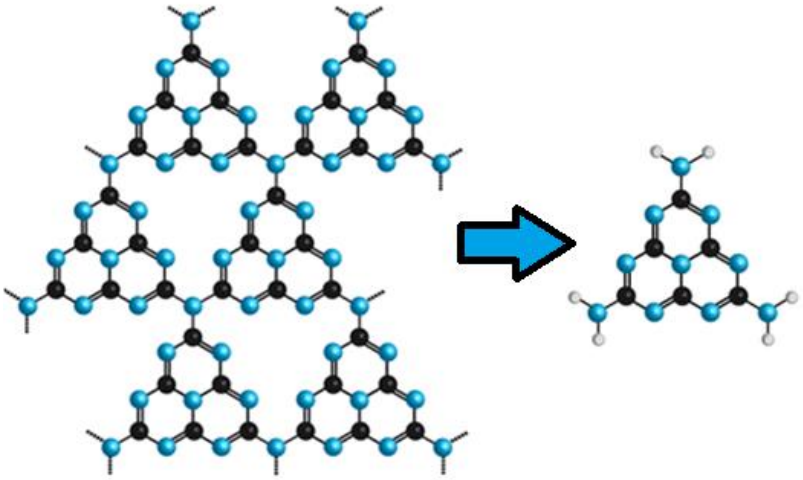

Figure 03 :Molecular Structure of s- Heptazine unit

The interlayer distance between the stacked sheets is typically around 0.326 nm, slightly larger than that of graphite (0.335 nm) due to the presence of nitrogen atoms. Real g-C_3N_4 materials often contain defects, such as nitrogen vacancies, carbon vacancies, and uncondensed amino groups, which can influence their properties[63].

I.6.2 Crystalline Forms of graphite carbon nitride g-C_3N_4

Beyond the commonly studied graphitic form, g-C3N4 can exist in several other crystalline structures, each with distinct atomic arrangements and properties. These include[57]:

1. α-C_3N_4: This phase has a hexagonal crystal structure characterized by alternating carbon and nitrogen atoms.

2. β-C_3N_4: This phase exhibits a trigonal crystal structure with a unique atomic arrangement.

3. **Cubic-C_3N_4:** This form has a cubic crystal structure, providing a symmetrical arrangement of carbon and nitrogen atoms.

4. **Pseudocubic-C_3N_4:** Similar to the cubic structure but with slight distortions, making it not perfectly cubic.

I .6.3 Chemical and Physical Properties of Graphitic Carbon Nitride (g-C_3N_4)

One of its most notable chemical properties is its excellent chemical stability, which allows it to resist degradation in strong acids, bases, and oxidizing environments. The high thermal stability, with g-C_3N_4 able to withstand temperatures up to 600°C without significant decomposition. This thermal robustness makes it suitable for high-temperature applications like catalysis and energy storage, where materials are often subjected to extreme conditions[64]. This stability is attributed to the strong covalent bonds between carbon and nitrogen atoms, forming a robust network that maintains its integrity even under harsh chemical conditions. This property makes g-C_3N_4 durable for long-term applications in various chemical processes[65].

The presence of nitrogen atoms in the structure of g-C_3N_4 imparts an electron-rich nature to the material. This electron density is due to the lone pair electrons on the nitrogen atoms, which contribute to the formation of a highly delocalized π-conjugated system. This electron-rich nature enhances the material's basic surface functionalities and hydrogen-bonding motifs,

making it effective in catalytic and electronic applications where electron transfer processes are critical.[66]

g-C_3N_4 is also an effective visible-light photocatalyst, capable of driving various reactions such as water splitting, CO_2 reduction, and the degradation of organic pollutants. Its photocatalytic activity is primarily due to its suitable band gap of approximately 2.7 eV, which allows it to absorb visible light and generate electron-hole pairs. The material's high surface area and the presence of active sites further enhance its photocatalytic efficiency by facilitating the interaction with reactants and inhibiting the recombination of photogenerated electron-hole pairs. This band gap is crucial for applications such as photocatalytic hydrogen production, water splitting, CO_2 reduction, and organic pollutant degradation[67].

g-C_3N_4 can act as a metal-free catalyst for various reactions, including NO decomposition, oxidation reactions, and organic transformations. This property is particularly beneficial for applications where the use of metals is undesirable due to cost or environmental concerns. The material's catalytic activity is enhanced by its electron-rich nature and the presence of nitrogen atoms, which provide active sites for catalytic reactions[68].

g-C_3N_4 is capable of facilitating hydrogen evolution reactions, particularly when modified with other materials to enhance its photocatalytic efficiency. The material's ability to generate hydrogen from water under visible light irradiation makes it a promising candidate for sustainable energy applications. Modifications such as doping with metals or creating heterojunctions with other semiconductors can significantly improve the hydrogen evolution rate.[69]

g-C_3N_4 can intercalate lithium ions, making it a potential candidate for rechargeable battery applications due to its ability to store a large amount of lithium. This intercalation property is beneficial for energy storage applications where high capacity and stability are required. The material's layered structure and the presence of nitrogen atoms facilitate the intercalation process, enhancing its performance in lithium-ion batteries[70].

The elastic modulus of g-C_3N_4 has been reported to be in the range of 210 to 320 GPa, and its tensile strength ranges from 30 to 47 GPa, depending on the specific structure and synthesis method used. The hardness of g-C_3N_4 can reach up to 13 GPa, making it a very hard material[71].

Bulk g-C_3N_4 typically has a low specific surface area (<10 m^2/g), this can be significantly increased through structural modifications like creating mesoporous structures. Techniques such as nano-casting and template methods can increase the surface area, thereby enhancing the material's catalytic activity by providing more active sites.[72]

Graphitic carbon nitride also exhibits unique optical properties, including photoluminescence, which is useful for applications in bioimaging and sensing. Its optical phonon behavior, revealed by infrared and Raman spectroscopy, helps in understanding its electronic and vibrational properties.[73]

g-C_3N_4 has a density of approximately 2.3 g/cm^3, which is slightly higher than that of graphite due to the incorporation of nitrogen atoms into its structure. This higher density contributes to the material's mechanical strength and stability, which are advantageous for structural applications.[74]

I.7. Synthesis method of graphite carbon nitride g-C_3N_4

Melamine, a triazine-based compound with the chemical formula $C_3H_6N_6$, is commonly used in the production of plastics, adhesives, and laminates. It is a white crystalline substance known for its high nitrogen content and thermal stability. Due to these properties, melamine serves as an excellent precursor for the synthesis of graphitic carbon nitride (g-C_3N_4)[75].

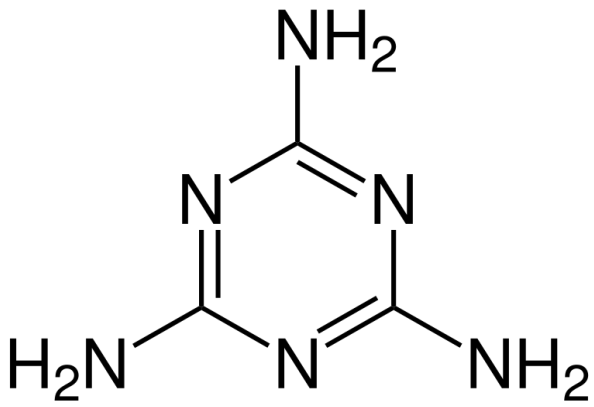

Figure 04:Molecular Structure of Melamine

To synthesize g-C_3N_4, melamine powder, initially white in color, undergoes a thermal treatment in a muffle furnace at 550°C for 2 hours. This process leads to the formation of g-C_3N_4, which exhibits a yellow color, indicating successful synthesis .And this is what it is called Calcination [76]

Calcination, the method used, is a thermal treatment process that involves heating a material to a high temperature in the absence of air or in a controlled atmosphere to bring about thermal decomposition, phase transition, or the removal of volatile substances[77].

Graphitic carbon nitride (g-C_3N_4) can be synthesized using various methods, each employing distinct precursors and conditions. These methods encompass thermal condensation/polymerization, solvothermal/ionothermal synthesis, template-assisted synthesis, mechanochemical synthesis, microwave-assisted synthesis, exfoliation/stripping methods, chemical vapor deposition (CVD), electrochemical/photochemical methods, biogenic synthesis, and hydrothermal synthesis[59].

The choice of precursor significantly influences the properties and yield of the resulting g-C_3N_4. Common precursors for g-C_3N_4 synthesis include urea ($CO(NH_2)_2$), cyanamide (CH_2N_2), dicyandiamide ($C_2H_4N_4$), and guanidine (CH_5N_3), among others. Each precursor, subjected to appropriate thermal treatments within the selected synthesis method, can lead to the formation of g-C_3N_4 with varying structural and morphological characteristics[78].

I.8. Modification of graphite carbon nitride g-C_3N_4

The modification of g-C_3N_4 with silver nanoparticles involves a careful balance of chemical reactions and process conditions to achieve the desired particle size and distribution. This modification enhances the catalytic properties of g-C_3N_4, making it a promising material for various environmental and industrial applications[79].

I.8.1 Silver nanoparticles

Silver nitrate ($AgNO_3$) is a widely used precursor in the synthesis of silver nanoparticles (AgNPs). It consists of silver cations (Ag^+) and nitrate anions (NO_3^-). When dissolved in water, $AgNO_3$ dissociates into these ions, making it an ideal source of silver for nanoparticle formation. Silver nanoparticles are particles of silver with dimensions typically ranging from 1 to 100 nanometers. These nanoparticles exhibit unique properties due to their high surface area to volume ratio and quantum effects, which differ significantly from bulk silver[80].

Silver nanoparticles are known for their excellent electrical conductivity, catalytic properties, and strong surface plasmon resonance (SPR) effects. The SPR effect enhances the absorption and scattering of light, making AgNPs highly effective in photocatalytic applications[81].

In the context of modifying g-C_3N4, silver nitrate serves as the source of silver ions that are adsorbed onto the surface and within the pores of the g-C_3N_4 matrix. This adsorption is a

critical step as it prepares the material for the subsequent reduction process, where the silver ions will be converted into metallic silver nanoparticles[82].

I.8.2 Reduction with Sodium Borohydride

Sodium borohydride ($NaBH_4$) is a powerful reducing agent commonly used in the synthesis of metallic nanoparticles. The reduction of silver ions (Ag^+) to metallic silver (Ag^0) using sodium borohydride. The borohydride ions (BH_4^-) donate electrons to the silver ions, reducing them to their metallic state[83]. This process is highly efficient and rapid, resulting in the formation of silver nanoparticles. The reduction typically occurs in an aqueous solution, where the silver ions are uniformly distributed, ensuring the formation of well-dispersed nanoparticles[84]. The use of sodium borohydride is advantageous due to its strong reducing power, which ensures complete reduction of silver ions. Additionally, the by-products of the reaction, such as boric acid ($B(OH)_3$), are relatively benign, making the process environmentally friendly.[85]

I.8.3. Chemical and Structural Implications of the modification

The modification of g-C_3N_4 with silver nanoparticles through the reduction of silver ions has several significant chemical and structural implications[86]

1. Enhanced Electron Conductivity: The incorporation of metallic silver nanoparticles into the g-C_3N_4 matrix significantly enhances its electron conductivity. Silver, being a highly conductive metal, facilitates the transfer of electrons within the composite material, which is crucial for catalytic and photocatalytic applications.[87]

2. Surface Plasmon Resonance (SPR) Effect: The silver nanoparticles exhibit strong SPR, which enhances the absorption of visible light. This effect extends the photocatalytic activity of g-C_3N_4 into the visible spectrum, making it more effective in light-driven catalytic processes.[82]

3. Improved Photocatalytic Activity: The presence of silver nanoparticles promotes the separation of photogenerated electron-hole pairs, reducing their recombination rate. This improvement leads to higher photocatalytic efficiency, as the electrons and holes can participate in redox reactions more effectively.[88]

4. Structural Stability: The modification process does not significantly alter the structural integrity of g-C_3N_4. The silver nanoparticles are well-dispersed on the surface and within the pores, maintaining the overall stability and surface area of the material. This dispersion

ensures that the catalytic sites are readily accessible, enhancing the overall performance of the composite[89].

5. Chemical Interactions: The interaction between the silver nanoparticles and the g-C_3N_4 matrix can lead to the formation of new active sites, which can further enhance the catalytic properties of the composite. These interactions are often characterized by techniques such as X-ray photoelectron spectroscopy (XPS) and Fourier-transform infrared spectroscopy (FTIR), which provide insights into the chemical bonding and electronic structure of the modified material.[90]

I.9.Heterogeneous Catalysis

Heterogeneous catalysis represents a fundamental process in both environmental and industrial applications, where the catalyst and reactants are in different phases, typically with the catalyst being solid and the reactants being in a liquid or gaseous state. This distinction allows for the catalyst to be easily separated from the reaction mixture, making heterogeneous catalysis particularly appealing for continuous industrial processes[91]. The essence of heterogeneous catalysis lies in the interaction between the surface of the solid catalyst and the reactant molecules. These interactions facilitate chemical reactions by providing an alternative reaction pathway with a lower activation energy compared to the uncatalyzed process[92]. The surface of the catalyst offers active sites where these reactions can occur more readily. The effectiveness of a heterogeneous catalyst is largely determined by its surface area; a higher surface area provides more active sites for the reactant molecules, thereby enhancing the catalytic activity[93].

Graphitic carbon nitride (g-C_3N_4), has emerged as a promising material for heterogeneous catalysis due to its unique structural and chemical properties. The modification of g-C_3N_4, through processes such as doping with metal nanoparticles or combining with other semiconductors, can significantly enhance its catalytic performance. These modifications can introduce new active sites, improve charge separation and transfer, and extend the light absorption range, making g-C_3N_4 based composites highly effective for various catalytic applications[94].

In environmental remediation, g-C_3N_4 based catalysts have shown remarkable efficiency in the degradation of organic pollutants under light irradiation, showcasing their potential in photocatalytic applications. The ability of these catalysts to facilitate the breakdown of complex organic molecules into less harmful substances under ambient conditions highlights

the role of heterogeneous catalysis in addressing pollution and environmental sustainability[6].

g-C_3N_4 based materials have been explored for their potential in energy conversion processes, such as hydrogen evolution from water splitting and carbon dioxide reduction. These applications leverage the photocatalytic properties of g-C_3N_4, where the material acts as a heterogeneous catalyst to drive the conversion of water and carbon dioxide into valuable fuels using sunlight[95].

The exploration of g-C_3N_4 in heterogeneous catalysis opens up new avenues for the development of efficient and sustainable catalytic processes. By tailoring the properties of g-C_3N_4 through various modification strategies, it is possible to design catalysts that are not only highly active but also selective for specific reactions. This adaptability, combined with the environmental benignity and cost-effectiveness of g-C_3N_4, positions it as a promising material for future advancements in catalysis and environmental remediation.

I.10.Catalytic reduction

Catalytic reduction plays a crucial role in environmental chemistry, particularly for treating pollutants in wastewater. This process uses a catalyst to accelerate the reduction of harmful substances into less toxic or non-toxic forms. Widely applied in degrading pollutants like dyes, heavy metals, and organic compounds found in industrial effluents, catalytic reduction is efficient and can be conducted under mild conditions, making it suitable for large-scale environmental applications[96].

In catalytic reduction, a catalyst facilitates electron transfer from a reducing agent to the pollutant, lowering the activation energy and increasing the reaction rate without being consumed. The general mechanism involves adsorption of pollutant molecules and reducing agents onto the catalyst, electron transfer, and desorption of reduced products, regenerating active sites for further reactions[97].

I.10.1. Catalytic reduction types

The efficiency of catalytic reduction depends on the nature of the catalyst and the reaction conditions. Common catalysts include noble metals (e.g., platinum, palladium, silver), metal oxides, and supported metal nanoparticles. These catalysts provide active sites for the adsorption and reduction of pollutants[98].

1. **Noble Metal Catalysts:** Noble metals like platinum and palladium are highly effective in catalytic reduction due to their excellent electron transfer capabilities and stability. However, their high cost limits their widespread use.[99]
2. **Metal Oxide Catalysts**: Metal oxides such as titanium dioxide (TiO_2) and zinc oxide (ZnO) are cost-effective alternatives with good catalytic properties. They are often used in combination with other materials to enhance their performance[100].
3. **Supported Metal Nanoparticles**: Supporting metal nanoparticles on materials like carbon, silica, or g-C_3N_4 can significantly enhance their catalytic activity. The support material provides a high surface area and stability, while the metal nanoparticles offer active sites for the reduction reactions[101].

10.2. Catalytic Reduction of Dyes

Catalytic reduction is a vital process in the treatment of dye pollutants in wastewater. This method involves the use of a catalyst to accelerate the reduction of dye molecules, transforming them into less toxic or non-toxic forms. The process is particularly effective for the degradation of synthetic dyes, which are commonly used in various industries such as textiles, leather, and paper. These dyes are often resistant to biodegradation and can cause significant environmental pollution if not properly treated[102].

- **Reduction of Methylene Blue**

Methylene blue (MB) is a synthetic dye with the chemical formula $C_{16}H_{18}N_3SCl$. It is widely used in various applications, including as a staining agent in microbiology and as a medication. Methylene blue is known for its vibrant blue color and its stability, which makes it a persistent pollutant in wastewater. Its structure consists of two aromatic benzene rings connected by a central phenothiazine ring containing nitrogen (N) and sulfur (S) atoms. This structure includes a nitro group (-NO_2) and a methyl group (-CH_3), contributing to its chemical functions as a dye and redox agent[103].[104]

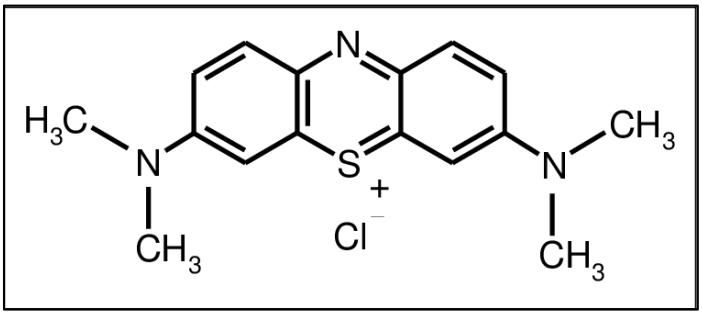

Figure 05 : Molecular structure of methylene blue

The reduction of methylene blue is a chemical process that transforms it into a less toxic and colorless form, making it easier to remove from the environment. When methylene blue is reduced, the nitro group ($-NO_2$) present in its structure is converted into an amine group NH_2 This reduction process involves the loss of oxygen atoms from the nitro group, which are replaced by hydrogen atoms to form the amine group. The reduction typically occurs in two main steps[105] first, the formation of a nitroso group (-NO) where the nitro group ($-NO_2$) initially loses an oxygen atom and gains an electron to form a nitroso group (-NO), which is an unstable radical[106].

second, the formation of an amine group ($-NH_2$) where the nitroso group (-NO) is further reduced by accepting another electron, often provided by the reducing agent, to form the amine group ($-NH_2$).

Sodium borohydride ($NaBH_4$) acts as the reducing agent, donating electrons to the methylene blue molecules. The catalyst facilitates this electron transfer, leading to the reduction of methylene blue to leuco-methylene blue, a colorless and less toxic form. The conversion of the nitro group to an amine group results in significant changes in the chemical structure and properties of methylene blue. There is a change in functional groups as the nitro group ($-NO_2$) is an oxidized functional group, while the amine group ($-NH_2$) is a reduced functional group[107].

The reduction process involves replacing the oxygen atoms in the nitro group with hydrogen atoms in the amine group, changing the compound's chemical reactivity and its interactions with other molecules[108]. There is also a change in electrical charge and polarity as the replacement of the oxygen atoms with hydrogen atoms in the amine group alters the electrical charge distribution and polarity of the molecule. The nitro group is highly polar and contributes to the overall polarity of methylene blue, whereas the amine group is less polar, affecting the solubility and interaction of the reduced molecule with its environment.[109]

Additionally, the reduction of methylene blue leads to a color change from dark blue to colorless or a lighter shade. This color change is due to the transformation of the double bonds between carbon and nitrogen (-N=C-) and ($-C=N^+(CH_3)_2$) into single bonds (-NH-CH-) and ($-CH-HN^+(CH_3)_2$), respectively. The reduction disrupts the conjugated system of double bonds, which is responsible for the dye's color[110]. Lastly, the reduction alters the solubility and chemical properties of methylene blue, making it less toxic and easier to remove from industrial

effluents. The reduced form, leuco-methylene blue, is less likely to interact with biological systems and cause environmental harm[103].

- **Reduction of Azo dyes Methyl orange**

Azo dyes are a class of synthetic dyes characterized by the presence of one or more azo groups (-N=N-) that link aromatic rings. These dyes are widely used in various industries, including textiles, leather, and food, due to their vibrant colors and stability[111]. Methyl orange is an example of an azo dye with the chemical formula $C_{14}H_{14}N_3NaO_3S$. It is commonly used as a pH indicator in titrations due to its clear color change from red in acidic conditions to yellow in alkaline conditions. The structure of methyl orange includes an azo group (-N=N-) that links two aromatic rings, which is responsible for its vivid color. Azo dyes like methyl orange are known for their stability and resistance to biodegradation, making them persistent pollutants in wastewater[112].

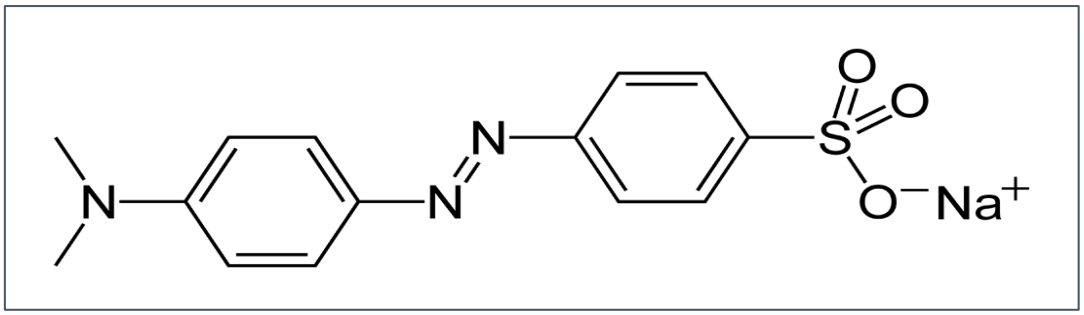

Figure 06: Molecular structure of methyl orange

The reduction mechanism involves the cleavage of the azo bond (-N=N-) and its conversion into amine groups ($-NH_2$) through two main steps: the formation of a hydrazine intermediate (-NH-NH-) and its subsequent reduction to amine groups ($-NH_2$). This process significantly alters the chemical structure and properties of methyl orange. The conversion of the oxidized azo group to reduced amine groups changes the molecule's chemical reactivity and interactions[113]. Additionally, the shift from a highly polar azo group to less polar amine groups affect the molecule's solubility and interaction with its environment. A noticeable color change occurs during reduction, from bright orange to colorless or a lighter shade, due to the disruption of the conjugated double bond system responsible for the dye's color. This alteration enhances the solubility and reduces the toxicity of methyl orange, facilitating its removal from industrial effluents[114]

Table 02 :Chemical Structures of Dyes and Their Reduced Forms

Dye Name	Chemical Structure	Reduced Form Structure
Methylene Blue	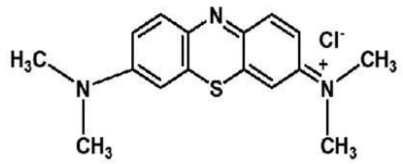	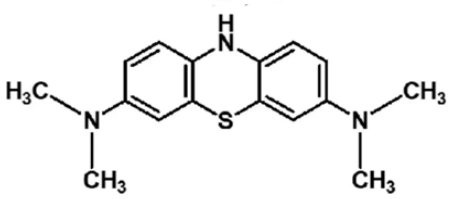
Methyl orange	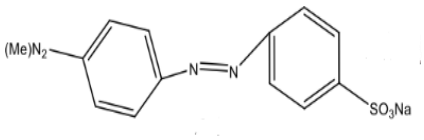	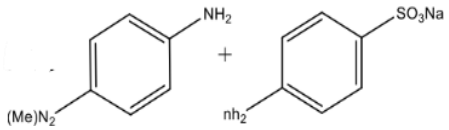
Congo Red	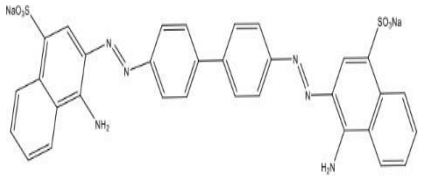	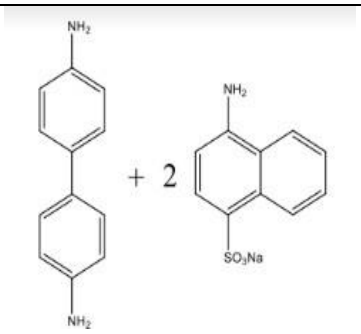
Orange G	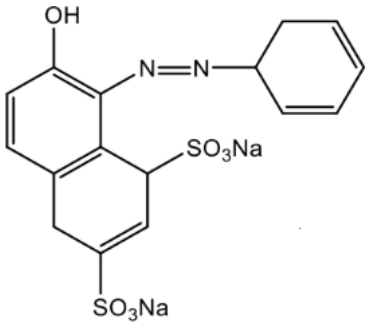	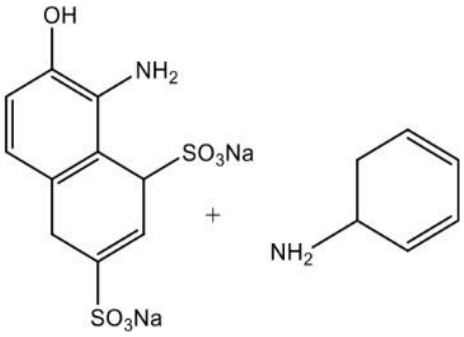
4-Nitrophenol		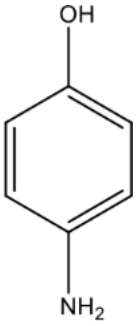

I.11.Factors Influencing the Efficiency of Pollutant Reduction

The efficiency of reducing pollutants such as methylene blue and Orange G depends on several critical factors. These include the initial amount of pollutant, the quantity and concentration of the reducing agent, the pH and temperature conditions of the reaction, and the presence of catalysts. Careful optimization of these factors is essential for achieving the highest possible reduction efficiency.[115]

By carefully considering and optimizing these factors, the reduction process for pollutants can be made more efficient, leading to more effective treatment and better environmental outcomes.

- **Initial Pollutant Amount**

The initial amount of the pollutant is crucial in determining the reduction efficiency. Generally, a higher pollutant concentration requires a larger quantity of reducing agent to achieve complete reduction. This is because the reduction reaction relies on the available reducing agent. If the initial pollutant concentration is excessively high, the available reducing agent may be insufficient, resulting in incomplete reduction. Therefore, balancing the initial pollutant concentration is key to ensuring efficient reduction[116].[117]

- **Quantity of Reducing Agent Applied**

The amount of reducing agent applied must be sufficient to ensure complete reduction of the pollutant without being excessive. An insufficient quantity of the reducing agent will not achieve full reduction, while an excessive amount can lead to undesirable effects, such as increased production of hydrogen gas. Thus, determining the optimal amount of reducing agent is vital for effective pollutant reduction[118].

- **Reducing Agent Concentration**

The concentration of the reducing agent is another critical factor. Higher concentrations can accelerate the reduction reaction, enhancing efficiency. However, excessively high concentrations can lead to unwanted side effects, such as the formation of byproducts. Therefore, it is essential to optimize the concentration of the reducing agent to achieve the best reduction results without causing adverse effects[119].

- **pH Conditions**

The pH level of the reaction environment significantly impacts pollutant reduction. The pH can influence the solubility of the pollutant, the stability of the reducing agent, and the reaction kinetics. Optimal pH conditions vary depending on the specific pollutant and reducing agent used. Adjusting the pH to the ideal level for each reaction can greatly improve reduction efficiency[120].

- **Temperature Conditions**

Temperature plays a significant role in the reduction process. Higher temperatures can accelerate the reaction by providing the necessary activation energy. However, very high temperatures can cause excessive evaporation of the solvent and produce unwanted byproducts, such as increased hydrogen gas. Lower temperatures, on the other hand, may slow down the reaction but can help minimize adverse side effects. Therefore, maintaining an optimal temperature is crucial for efficient pollutant reduction[121].

- **Catalytic Agents**

The presence of catalytic agents can significantly enhance the reduction of pollutants. Catalysts lower the activation energy required for the reaction, thereby speeding up the process. Commonly used catalysts in pollutant reduction include iron, palladium, and platinum. Catalysts also affect the selectivity of the reduction process, potentially leading to the formation of different products. Incorporating the right catalyst can greatly improve the efficiency and outcome of the reduction reaction[122].

I.12.Characterization Techniques

- **X-ray Diffraction (XRD)**

X-ray Diffraction (XRD) is a technique used to determine the crystal structure and phase composition of materials. It involves directing X-rays at a sample and measuring the intensity and angles of the diffracted beams. crystallinity of materials.[123]

- **Fourier-Transform Infrared Spectroscopy (FTIR)**

Definition: Fourier-Transform Infrared Spectroscopy (FTIR) is a technique used to identify functional groups and chemical bonds in a compound by measuring the absorption of infrared radiation at different wavelengths. The resulting spectrum represents the molecular fingerprint

of the material, showing characteristic absorption peaks corresponding to specific bond vibrations. FTIR is widely used to analyze organic and inorganic compounds, identify unknown substances, and study molecular interactions and chemical compositions.[124]

- **UV-Vis Spectrophotometry**

UV-Vis Spectrophotometry is a technique used to measure the absorbance of ultraviolet (UV) and visible (Vis) light by a sample. The absorbance spectrum provides information about the electronic transitions in molecules, which can be related to the concentration and chemical composition of the sample. UV-Vis Spectrophotometry is commonly used to quantify the concentration of substances in solution, monitor chemical reactions, and study the optical properties of materials.[125]

Conclusion

In conclusion, Chapter I has provided a thorough bibliographic study of the key materials and concepts underpinning this research. We have examined the properties and synthesis methods of g-C_3N_4, its modifications to enhance catalytic performance, and the characterization techniques essential for analyzing these materials. This foundational knowledge is crucial for understanding the experimental approaches and results presented in the following chapters.

METHODES AND MATERIALS

I.Introduction

This chapter details the experimental methodologies and materials utilized in this research to synthesize and modify graphitic carbon nitride (g-C3N4) for catalytic applications. The primary materials used include melamine, silver nitrate, and sodium borohydride, each serving a specific purpose in the synthesis and modification processes. The synthesis of g-C3N4 from melamine involves a calcination process, while the modification steps incorporate silver nitrate and sodium borohydride to enhance the catalytic properties of the composite. These procedures are meticulously designed to ensure the successful formation of silver-modified g-C3N4, which is subsequently characterized using various techniques to validate its structure and functionality. The experimental setup, conditions, and observations are comprehensively documented to provide a clear understanding of the methodologies employed in this study.

II.1. Materials

Material	Formula	Molar Mass (g/mol)
Melamine	$C_3H_6N_6$	126.12
Silver Nitrate	$AgNO_3$	169.87
Sodium Borohydride	$NaBH_4$	37.83

II.2. Procedure and Observations

II.2.1. Synthesis of g-C_3N_4

Melamine, initially a white powder, was placed in a crucible and heated in a muffle furnace at 550°C for 2 hours. This process resulted in the formation of a yellow powder, indicating the successful synthesis of g-C_3N_4.

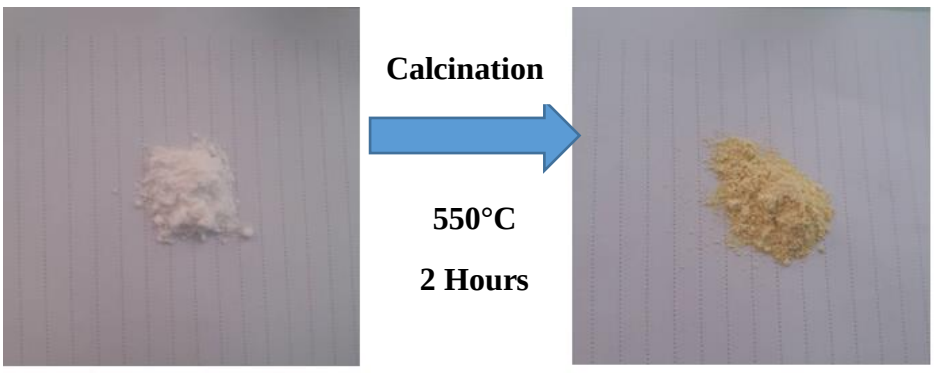

Figure 01: Melamine before and after the calcination

II .2.2. Modification of g-C3N4

II 2.2.1 Silver Nitrate

A 0.1 M solution of silver nitrate was prepared by dissolving 4.2 grams of silver nitrate in 250 ml of deionized water in a 500 ml beaker.

Six grams of g-C_3N_4 were then mixed with 200 ml of this solution in a separate beaker and stirred using a magnetic stirrer for two hours. The mixture turned yellow, suggesting the adsorption of silver ions onto the g-C_3N_4 surface. After filtration using a Büchner funnel and filter paper, the precipitate was dried in an oven at 60°C for 24 hours, resulting in a yellow powder of Ag@g-C_3N_4.

Figure 02: Modification of g-C3N4 with silver Nitrate

II .2.2.2 Sodium Borohydride

A 1 M solution of sodium borohydride was prepared by dissolving 3.75 grams of $NaBH_4$ in 100 ml of deionized water in a 250 ml beaker. Four grams of the yellow Ag@g-C_3N_4 powder were then added to 100 ml of this solution in a separate beaker and stirred using a magnetic stirrer for an hour and a half. The mixture turned black, indicating the reduction of silver ions to metallic silver Ag0. The final product, a black powder of Ag@g-C_3N_4, was obtained after filtration using a Büchner funnel and drying in an oven at 60°C for 24 hours.

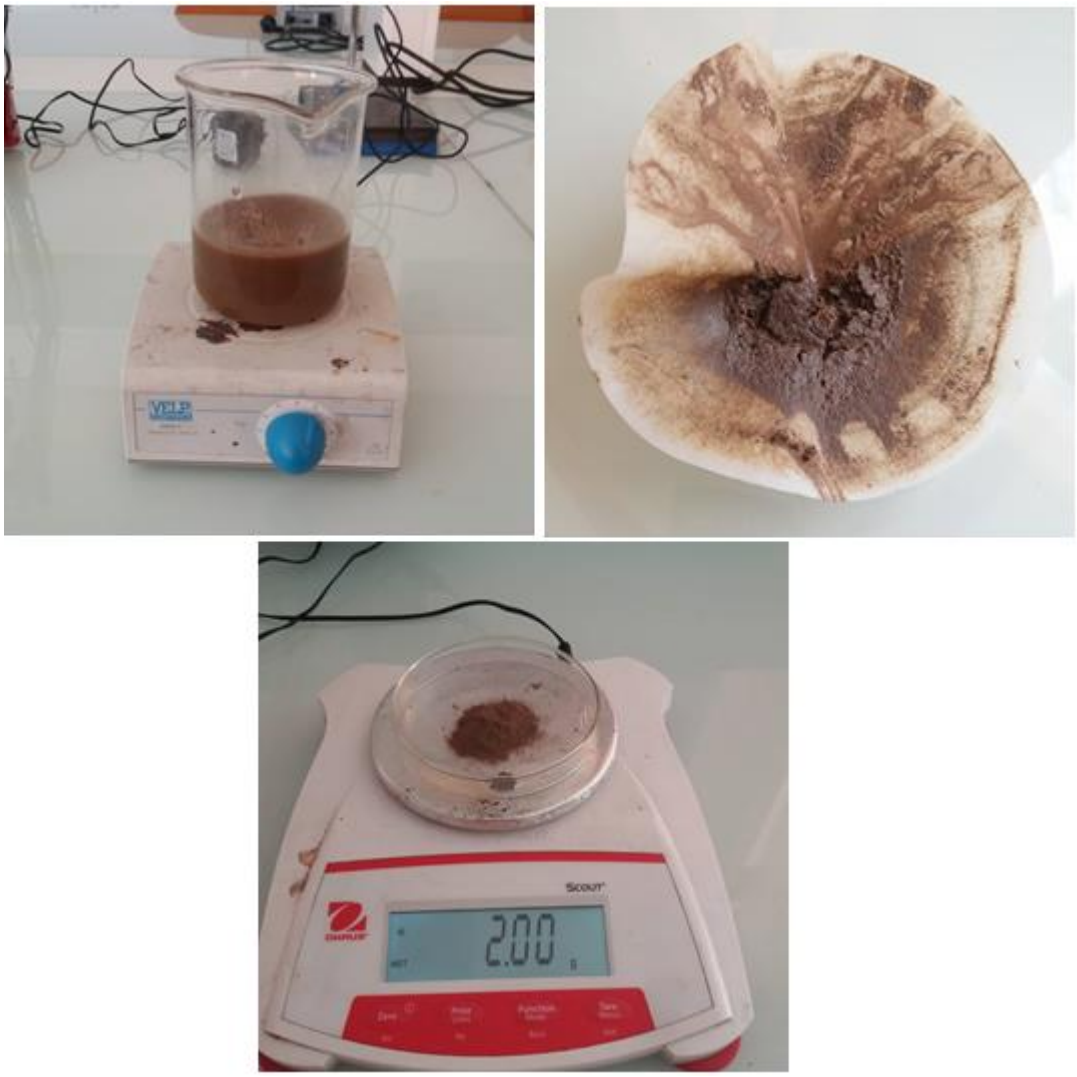

Figure 03: Modification of g-C3N4 with Sodium Borohydride

III. Characterization of materials

III.1.1.X-ray diffraction

X-ray diffraction patterns of the powder samples were collected using a D8 DISCOVER Plus diffractometer equipped with a Cu anticathode (λ Cu Kα anticathode = 0.154056 nm). Figure 01 shows the XRD spectra of the parent sample g-C_3N_4 and the nanocomposites Ag@g-C_3N_4. X-ray diffraction (XRD) is an essential technique for characterizing nanocomposites, providing crucial information on their crystal structure, composition and grain size. In this section, we present the results of the XRD characterization of the g-C_3N_4 sample and the Ag@g-C_3N_4 nanocomposites.

III.1.2. Principle of X-ray Diffraction

XRD is based on the interaction of X-rays with the crystalline planes of a material. When X-rays are directed at a sample, they are diffracted along the atomic planes of the crystal. The relationship between angle of incidence, X-ray wavelength and inter-plane distances is given by Bragg's law:

$$n\lambda = 2 \times d \times \sin\theta$$

Where n is the diffraction order, λ is the X-ray wavelength, d is the interplanar distance and θ is the angle of incidence.

III.1.3. Characterization of g-C_3N_4@CuO@AgO nanocomposites Identifying crystal phases

The XRD spectra of Ag@g-C_3N_4 nanocomposites show characteristic peaks corresponding to the crystalline phases of g-C_3N_4, and Ag0. The g-C3N4 diffraction peaks typically appear at angles 2θ° around 27.52° and 13.07°, corresponding to the (002) and (100) crystal planes respectively [126] confirms the formation of g-C_3N_4 by the thermal process. Ag0 peaks are detected at 2θ positions around 38°, 44°, 64° and 77°, attributable to the (111), (200), (220) and (311) planes. The X-ray diffractogram confirms the presence of silver nanoparticles[127] [128].

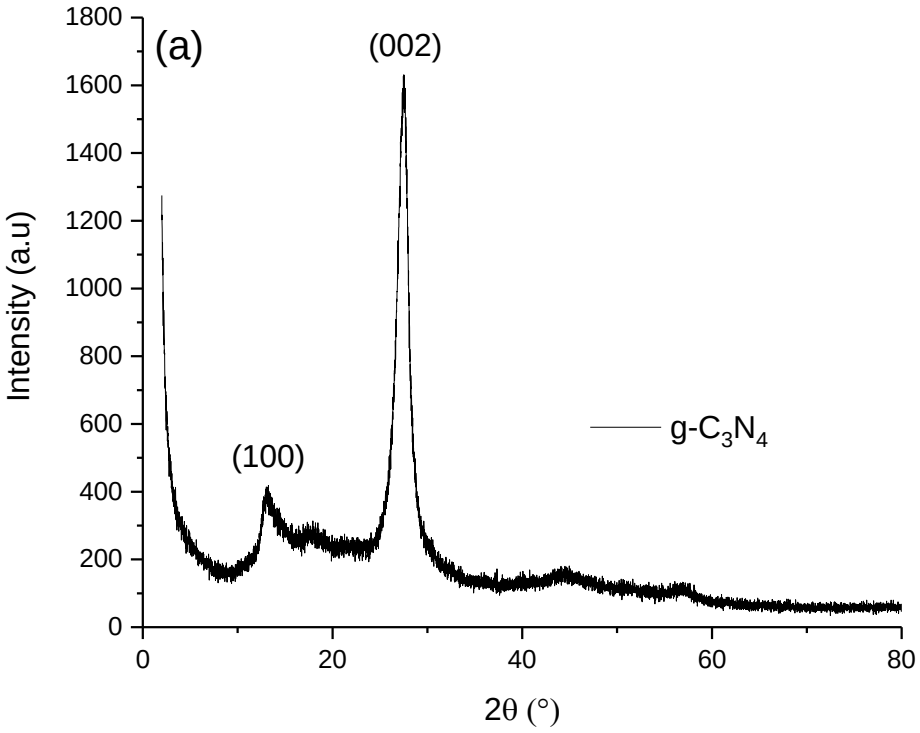

Figure 04: X-Ray Diffractogram of g-C3N4

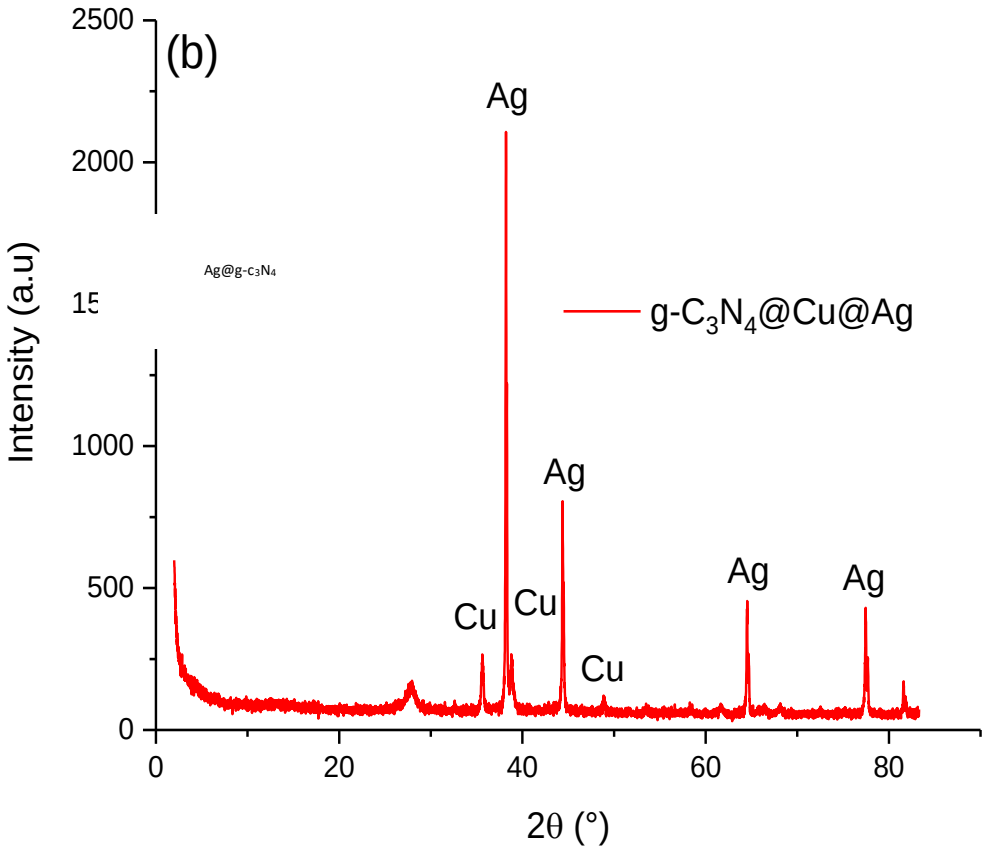

Figure 05: X-ray Diffractogram of Ag@g-C3N4

III.2.1 Infrared spectroscopy

Characterization of Nanocomposites by Fourier Transform Infrared Spectroscopy (FTIR) are shown in Figure 03. Fourier Transform Infrared Spectroscopy (FTIR) is an essential analytical technique for determining the functional groups and chemical bonds present in nanocomposites. In this section, we present a detailed analysis of the FTIR spectra of the g-C_3N_4 sample and the Ag@g-C_3N_4 nanocomposites.

III.2.2. Principle of FTIR Spectroscopy

FTIR measures the absorption of infrared light by chemical bonds within a material. Each type of chemical bond absorbs at specific frequencies, making it possible to identify functional groups and study interactions between material components[129].

III.2.3. Characterization of Ag@g-C_3N_4 nanocomposites FTIR spectrum of g-C_3N_4

Graphitic carbon nitride (g-C_3N_4) displays characteristic absorption bands in the FTIR spectrum. Bands between 1200 and 1700 cm^{-1} correspond to valence vibrations of the C=N and C-N-C bonds, typical of the triazine lattice of g-C_3N_4. An intense band around 810 cm^{-1} is attributed to out-of-plane deformation vibrations of the triazine rings.

III.2.4. FTIR spectrum of Ag@g-C_3N_4 nanocomposites

The characteristic g-C_3N_4 bands are present, confirming the conservation of the basic g- C_3N_4 structure after nanocomposite formation. New bands appear around 500-600 cm^{-1}, corresponding to the valence vibrations of Ag-O bonds. These bands indicate the presence of Ag 0 in the nanocomposites. The band around 1380 cm^{-1}, often associated with the symmetrical vibration of nitride groups (C-N), may be slightly shifted due to interactions between g-C_3N_4 and Ag0.

III.2.5. Interactions and Structural Modifications

Shifts in absorption bands and the appearance of new bands suggest chemical interactions between g-C_3N_4 and Ag nanoparticles. Changes in the vibrational bands of the C=N and C-N-C groups indicate a strong interaction between g-C_3N_4 and the nanoparticles, influencing the electronic and catalytic properties of the nanocomposites.

The FTIR spectra of Ag@g-C_3N_4 are shown in Figure 03. The FTIR characteristics of g-C_3N_4 are similar to those described above, with bands between 1200 and 1700 cm-¹ for C=N and C-N-C bonds, and a band at 810 cm-¹ for triazine rings.

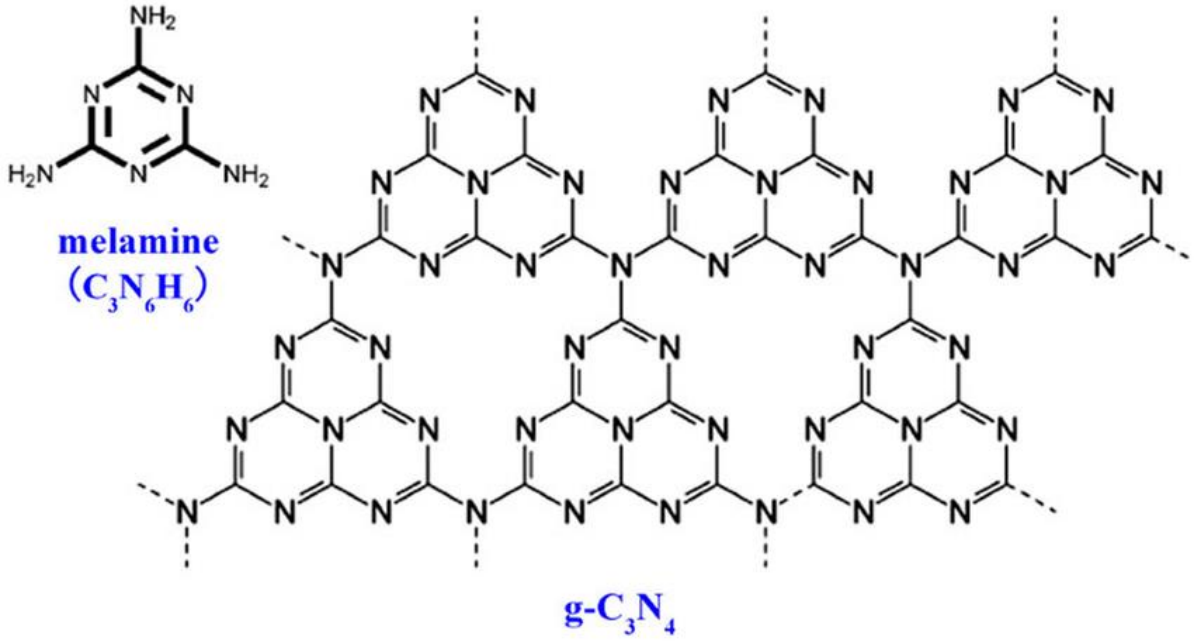

Figure 06: Structure of melamine and g-C3N4

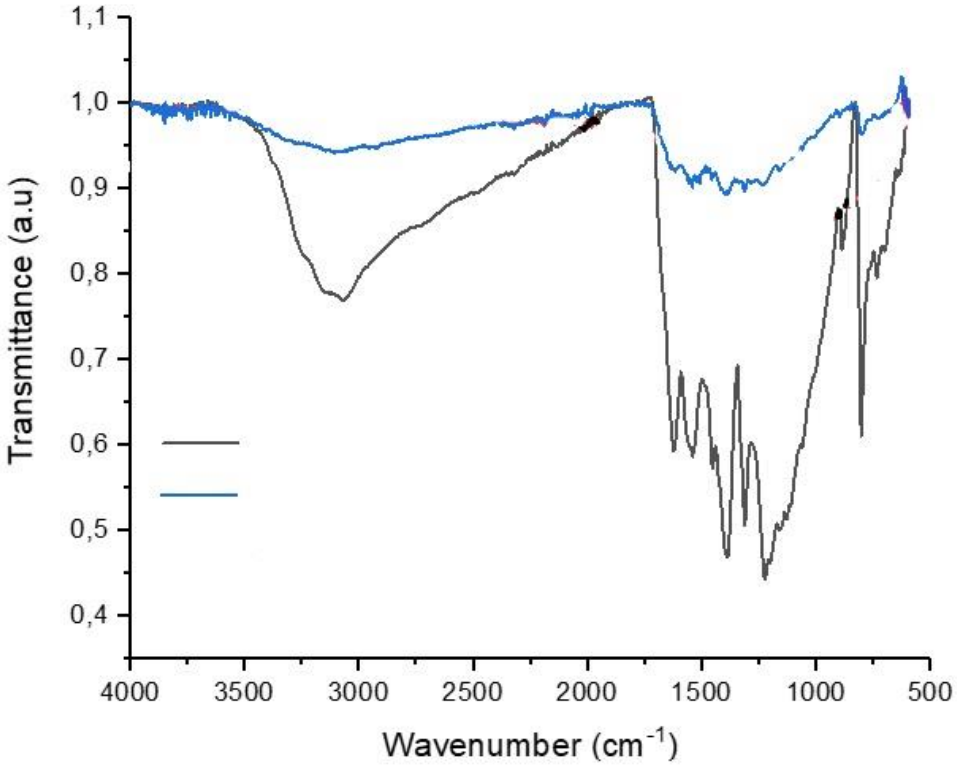

Figure 07: FTIR spectra of g-C3N4 and Ag@g-C3N4

IV. Application

IV.1. Catalytic reduction

The capacity of different catalysts was tested with two pollutants MB and MO in a simple binary system as model reactions. The synthesis protocol is similar to the work carried out in the literature, except that the conditions have been modified. Briefly, about 2 mL of MO solution (0.1mM) was placed in a quartz cuvette and a mass of catalyst (3 mg) was added to the mixture, after which 1.5 mL of freshly prepared $NaBH_4$ reducing agent (20-15 and 10 mM) was added to the reaction mixture. The reaction was monitored by UV-Vis using a scanning program every 30 seconds. The reduction of the MO dye was used as a model reaction to optimize the conditions of the reduction reaction. The best optimized conditions were used to reduce the MB dye. The conditions used were 0.1 mM MO, 20 mM $NaBH_4$, and 3 mg Ag@g-C_3N_4 catalyst. For the binary system MB + MO was studied using the same protocol, the conditions used were 0.05 mM MO, 0.05-0.025 mM MB, 0.1 mM $NaBH_4$ and 3 mg Ag@g-C_3N_4 catalyst.

IV.2. Effect of catalyst type

The catalytic activity of a material differs according to its surface, the nature of the active sites (metal NPs, metal oxides) their dispersions, but also the size of the MNPs. In this section, we are interested in studying the effect Ag@g-C_3N_4 nanoparticles on catalytic activity. Before studying the catalytic behavior of our materials, it is interesting to investigate the adsorption of our organic pollutants. As shown in figure 04, it is clear that the Ag@g-C_3N_4 catalyst has no adsorption affinity for the MO dye. After addition of the reducing agent $NaBH_4$ (see figure 04), it was found that the Ag@g-C_3N_4 catalyst gave more efficient results. A conversion of 80% of the MO dye was obtained for 210s under the following conditions: [MO] = 0.1 mM, [$NaBH_4$] = 15 mM, catalyst mass 3 mg. It should be borne in mind that the use of $NaBH_4$ alone (blank test without catalyst) does not lead to any conversion of the MO dye even at higher concentrations (between 15 and 20 mM). This shows that the presence of metal Ag supported on the surface of g-C_3N_4 plays an important role in MO dye conversion. According to the literature, it has been demonstrated that the role of Ag-CuNPs lies in the transport of electrons from the $NaBH_4$ donor to the acceptor (MO dye), which then leads to its conversion. The catalytic performance of this material compared with other catalysts lie in the number of sites available for reaction with the MO dye, as well as in their good dispersion and small size.

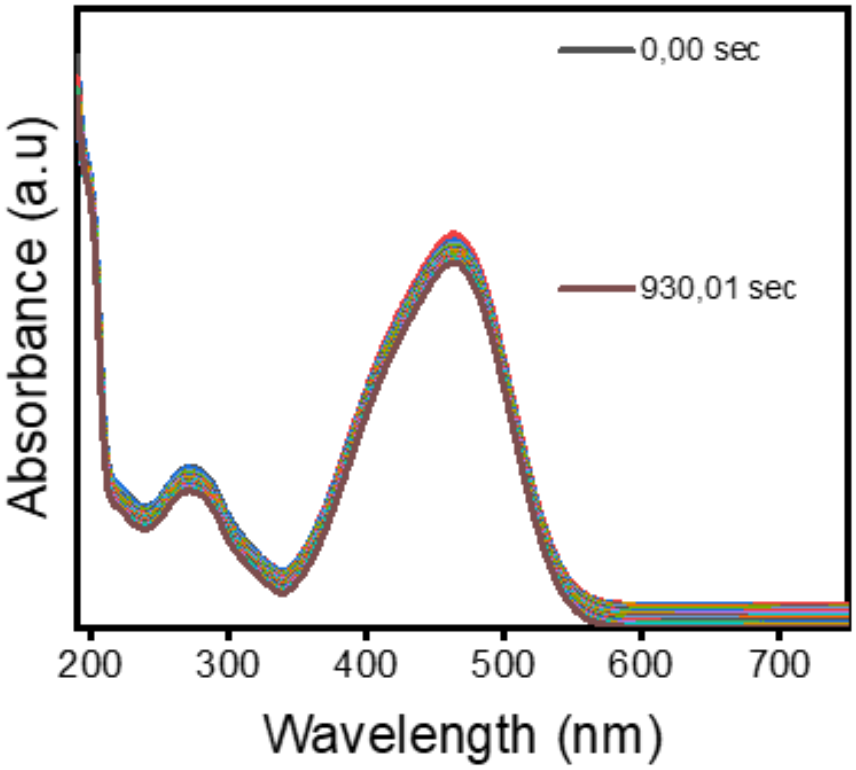

Figure 08: Uv-Vis Adsorption test on Ag@g-C3N4

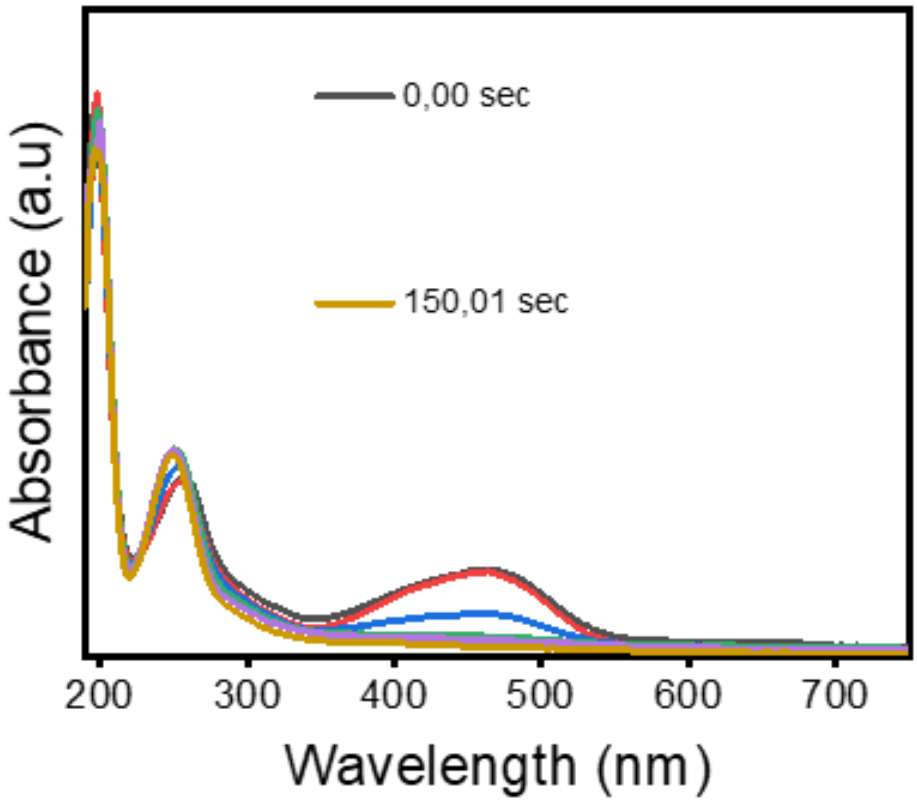

Figure 09: Reduction of Methyl Orange (MO)

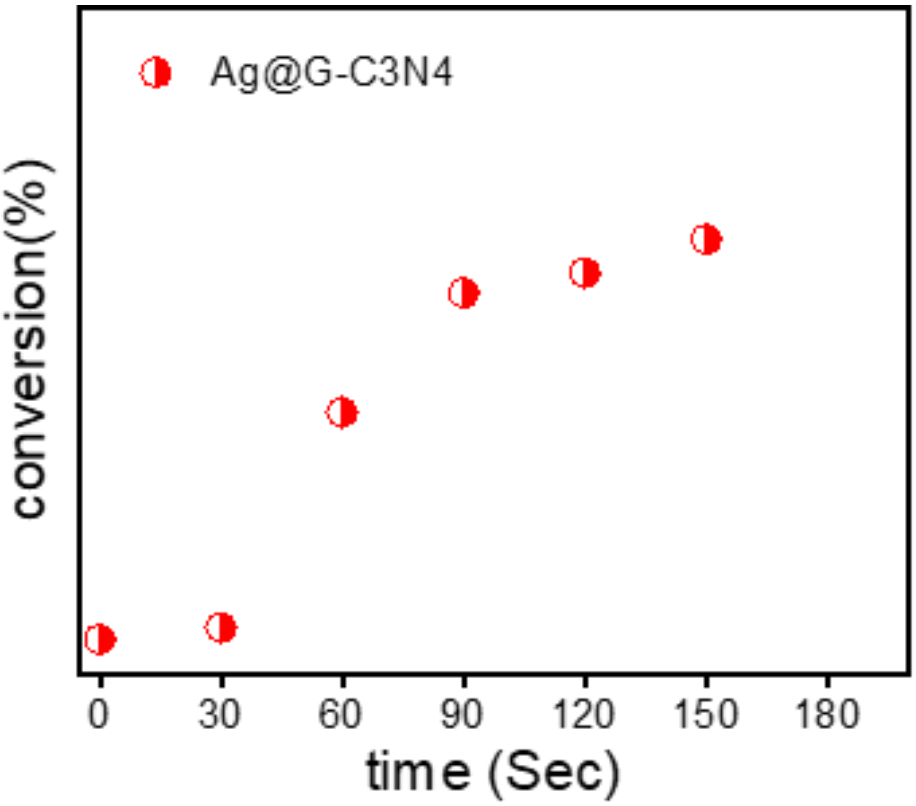

Figure 10: Conversion for the Reduction of MO

IV.3. Effect of $NaBH_4$ concentration

After optimizing the best catalyst, we studied the effect of $NaBH_4$ on MO dye conversion. To this end, we used different concentrations of $NaBH_4$ ranging from 10 to 20 mM while keeping the other conditions constant. As shown in Figure 05, the concentration of $NaBH_4$ caused a significant change, particularly in reaction time and thus in MO dye conversion. It is clear that MO dye conversion increases with increasing initial $NaBH_4$ concentration 4 and so the best MO conversion was obtained for 150s when using a $NaBH_4$ concentration of 20 mM. The rate constants recorded for $NaBH_4$ concentrations of 10, 15 and 20 mM are (0.005, 0.009) and (0.01 S -1), respectively. This is strongly related to the increase in electron density with increasing $NaBH_4$ concentration 4 which facilitates MO conversion.

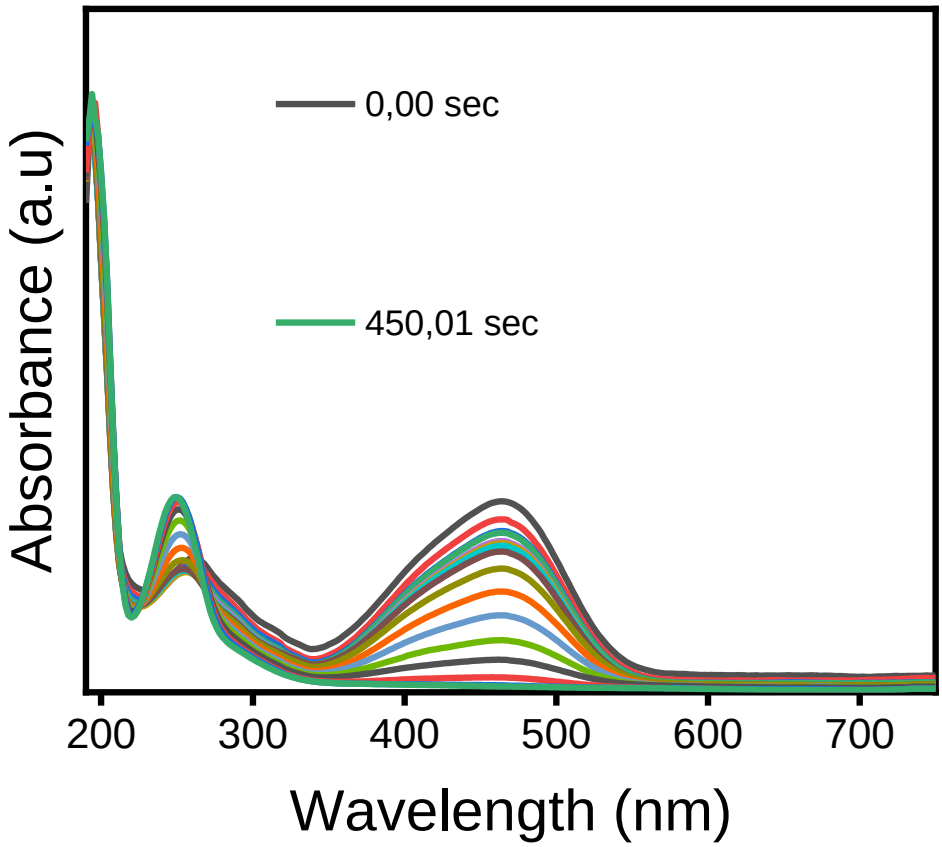

Figure 11: Effect of $NaBH_4$ Concentration (10mM)

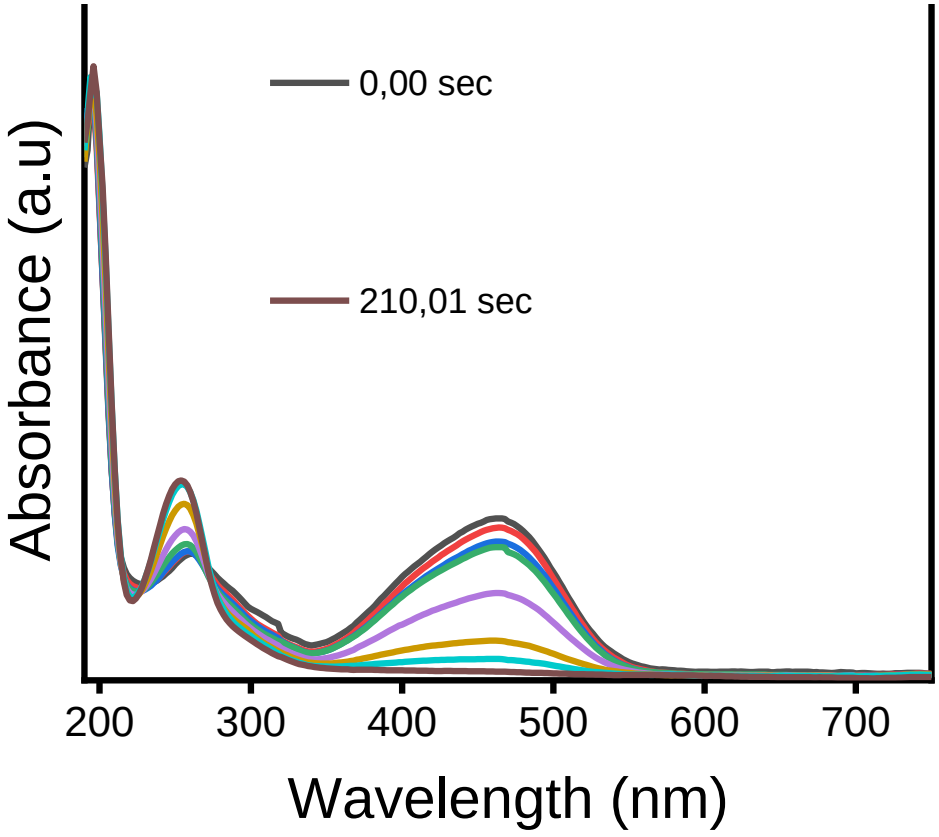

Figure 12: Effect of $NaBH_4$ Concentration (15mM)

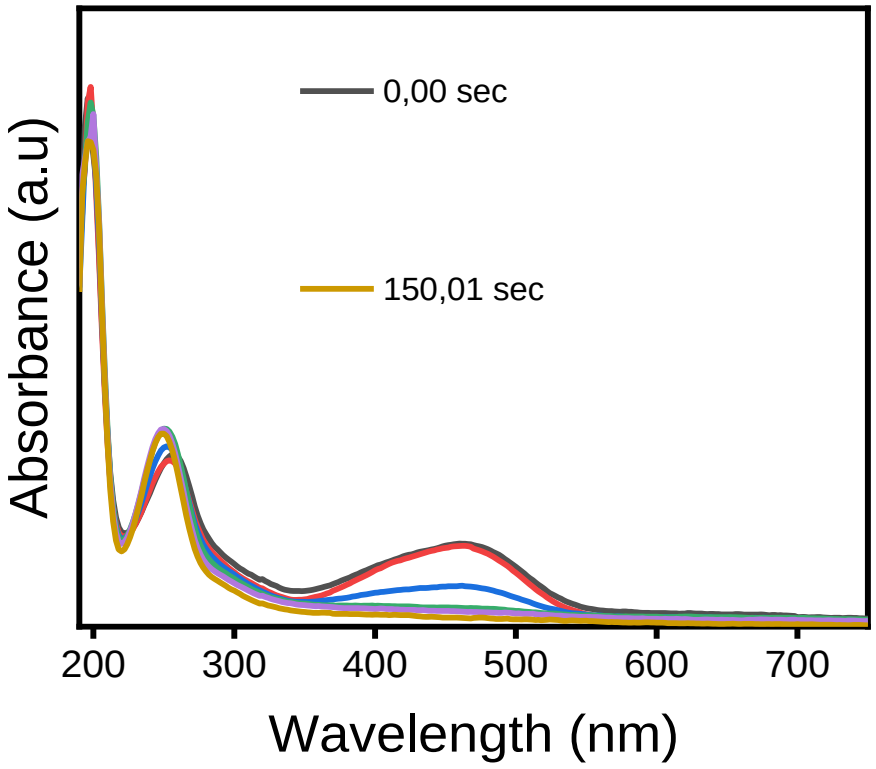

Figure 13: Effect of $NaBH_4$ Concentration (20mM)

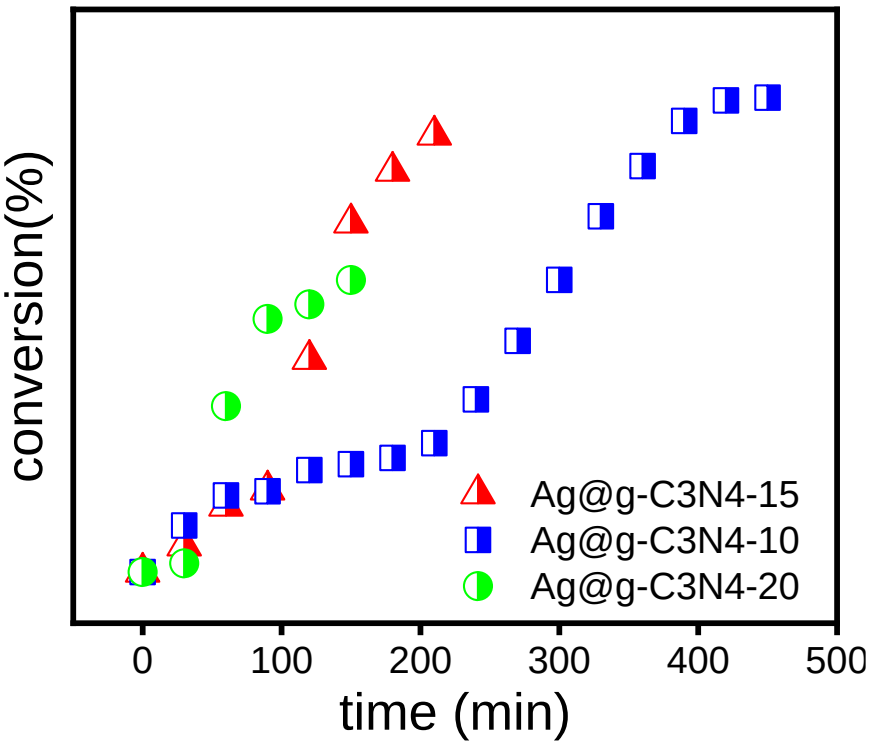

Figure 14: MO Conversion ($NaBH_4$ Effect)

IV.4. Effect of the nature of the organic pollutant

After optimizing the operating conditions (best catalyst and $NaBH_4$ concentration), we are now interested in studying the catalytic behavior of our Ag@g-C_3N_4 material in relation to the organic pollutant. The study of the catalytic behavior of our Ag@g-C_3N_4 material in relation to the cationic dye MB. The Ag@g-C_3N_4 catalyst showed excellent catalytic activity against this cationic pollutant. The Ag@g-C_3N_4 catalyst performed better with the MB dye, resulting in an instantaneous reaction, faster than for the reduction of MO. MB conversion was complete. Among the advantages of this material, it is easy to prepare and effective as a reducing agent.

IV.5. Reduction in a binary system

Organic pollutants can exist as a system containing one or more pollutants at the same time. This is why it is so important to test our material in a system containing several pollutants. To this end, we tested a binary system containing two different pollutants as model reactions. The system contained a mixture of MB dye and MO. The results obtained in the binary system are shown in Figure 15.

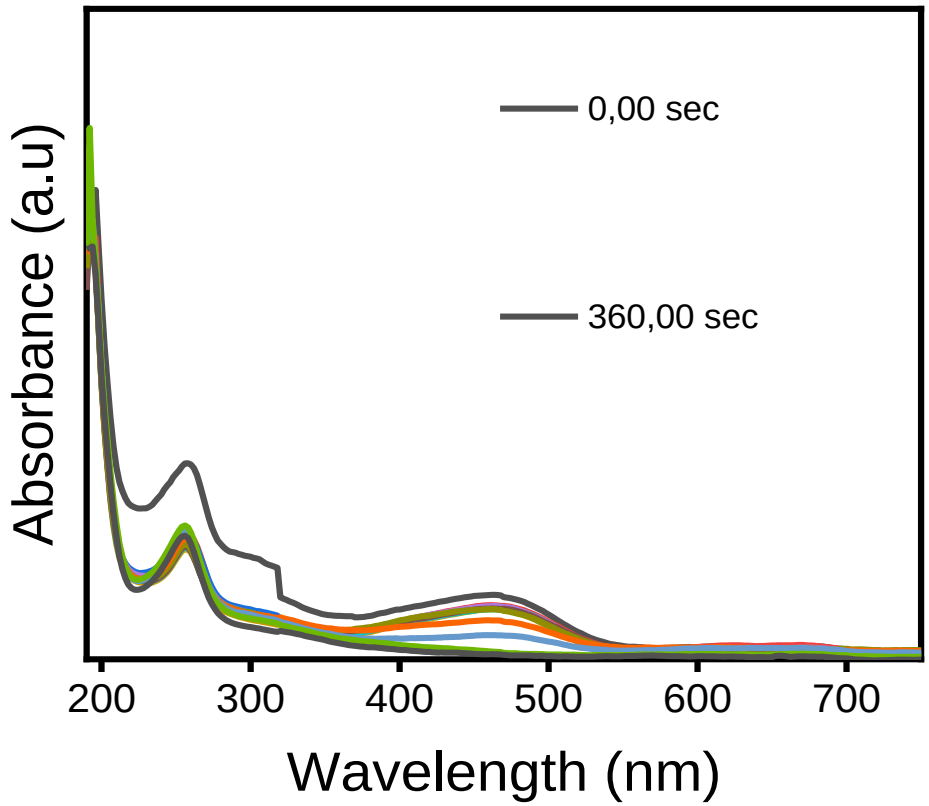

Figure 15: Uv-Vis Reduction spectrum of a MB-MO binary System using Ag@g-C3N4-20

From this figure, it is clear that our Ag@g-C_3N_4 catalyst performed well in this system. The Ag@g-C_3N_4 catalyst was more selective than the MB dye, which explains why the reaction time required to reduce MB was 90s, whereas for the MO dye, the reaction time was found to be four times that of MB, and the total conversion of the MO dye was around 360s.

Table 03:Comparative study with other catalysts

Catalyst	[BM]	[$NaBH_4$]	T (°C)	Catalyst Mass (mg)	Reaction Time (min)	Reference
Aerogel MC@CA (1)	0.6mM×2 mL	0.6 M×1.5 mL	Ta	4.8	5	[130]
MC-PDA-Ag	0.06mM×20 mL	0.01 M×2 mL	Ta	10	5	[131]
Ag/Fe_3O_4@C	0.06mM×18 mL	5.3mM×20 mL	Ta	10	10	[132]
CuO@CS	0.06mM×50 mL	1.5M×3.75 mL	Ta	25	10	[133]
Au/CeO_2–TiO_2	0.048mM×30 mL	0.2 M×2 mL	30	13	10.5	[134]
Cu/SBA-15	22.5 mL×0.09 mM +12.5 mL H_2O	0.2 M×5 mL	30	1	8	[135]
Au/TiO_2	0.04mM×20 mL	0.1 M×2 mL	Ta	2	12	[136]
CuO–SDS	0.6mM×2 mL	6.8mM×1.5 mL	Ta	3	10	[137]
CeO_2@ALG (2%)	0.3×1.5 mL	0.5M×2.5 mL	Ta	4	2	[138]
CeO_2@ALG (2%)	0.1×1.5 mL	0.1M×2.5 mL	Ta	4	15	[138]
KA	0.3mM×2 mL	15mM×1.5 mL	Ta	3	38	[139]
Ag@g-C_3N_4	0.1×2ml	20mM×1.5ml	25	3	2.5	This study

Conclusion

In this work, we prepared g-C_3N_4 from melamine. The material obtained is then used as a base material for the preparation of Ag@g-C_3N_4 nanocomposites. The nanocomposites obtained are characterized by X-ray powder diffraction and infrared spectroscopy (FTIR). Characterization of the Ag@g-C_3N_4 materials was carried out by X-ray diffraction (XRD) and infrared spectroscopy (IR) to determine their respective crystal structures and chemical bonds. XRD analysis revealed that catalyst possess a well-defined crystal structure, with characteristic peaks indicating the presence of g-C_3N_4 as well as Ag nanoparticles phases. IR spectroscopy confirmed the incorporation of Ag metals into the g-C_3N_4 matrix, showing bands specific to C=N and C-N bonds, as well as additional bands attributed to metal oxides. These structural and chemical characterizations confirmed the successful synthesis of the nanocomposites. Various parameters affecting the reduction of organic pollutants were studied and synthesis conditions were optimized. It was shown that the initial concentration of the reducing agent, as well as the nature of the dispersed NPs, can significantly influence the conversion of organic pollutants. According to our results, the Ag@g-C_3N_4catalyst was selected as the best catalyst in both systems (simple and binary). In the binary system, the Ag@g-C_3N_4 catalyst was more selective for the MB dye due to the perfect, ultra-fine dispersion of the (Ag) NPs particles. On the Ag@g-C_3N_4 surface. The Ag@g-C_3N_4 catalyst was shown to have excellent catalytic activity towards both pollutants (MO and MB)

General Conclusion

In this thesis, we have successfully synthesized and characterized graphitic carbon nitride (g-C_3N_4) and its silver-modified composites (Ag@g-C_3N_4) for catalytic applications in water purification. The experimental studies focused on the preparation of g-C_3N_4 from melamine and its subsequent modification with silver nanoparticles to enhance its catalytic efficiency. The characterization of these materials using X-ray diffraction (XRD) and Fourier-transform infrared spectroscopy (FTIR) confirmed the successful incorporation of silver nanoparticles into the g-C_3N_4 matrix, resulting in well-defined crystal structures and chemical bonds.

The catalytic performance of the synthesized Ag@g-C_3N_4 composites was evaluated through the reduction of organic pollutants, specifically methylene blue (MB) and methyl orange (MO) dyes. The results demonstrated that the Ag@g-C_3N_4 catalyst exhibited excellent catalytic activity towards both pollutants. Various parameters affecting the reduction process, such as the initial concentration of the reducing agent and the nature of the dispersed nanoparticles, were systematically studied and optimized. The Ag@g-C_3N_4 catalyst showed superior performance in both simple and binary systems, with a higher selectivity for the MB dye due to the ultra-fine dispersion of silver nanoparticles on the g-C_3N_4 surface.

The findings of this research highlight the potential of g-C_3N_4-based composites as effective and sustainable solutions for water pollution. The enhanced catalytic properties of Ag@g-C_3N_4 make it a promising candidate for environmental remediation applications, particularly in the degradation of harmful organic pollutants in wastewater.

this work has demonstrated the successful synthesis and application of g-C_3N_4 based composites for catalytic water purification. The insights gained from this research pave the way for further advancements in the design and application of advanced catalytic materials. We hope that this work will inspire future research and development in the field of environmental catalysis, ultimately leading to more efficient, cost-effective, and sustainable solutions for water pollution.

Through this work, we have contributed to the development of more effective and sustainable solutions for water pollution by leveraging the unique properties of g-C_3N_4 and its composites. The insights gained from this research pave the way for further advancements in the design and application of advanced catalytic materials for environmental remediation.

Looking ahead, future research directions could include further modifications to enhance the catalytic efficiency of g-C_3N_4, exploration of other pollutants and reaction systems, and the development of scalable synthesis methods for industrial-scale implementation.

Additionally, the integration of these materials into existing wastewater treatment processes and the assessment of their long-term stability and environmental impact would be crucial steps towards practical applications.

In conclusion, this thesis has made significant contributions to the field of catalytic materials for environmental remediation, highlighting the potential of g-C_3N_4 and its composites as promising solutions for addressing the pressing issue of water pollution. By combining fundamental research with practical applications, we have taken a step towards a more sustainable future, where advanced catalytic technologies play a pivotal role in preserving our precious water resources. As the famous environmentalist Robert Swan once said, "The greatest threat to our planet is the belief that someone else will save it.”. By advancing the field of material chemistry, we hope to contribute to the global effort of preserving our precious water resources and ensuring a healthier planet for future generations.

[1] N. Crini *et al.*, “Worldwide cases of water pollution by emerging contaminants: a review,” *Environ. Chem. Lett.*, vol. 20, Apr. 2022, doi: 10.1007/s10311-022-01447-4.

[2] L. Lin, H. Yang, and X. Xu, “Effects of Water Pollution on Human Health and Disease Heterogeneity: A Review,” *Front. Environ. Sci.*, vol. 10, Jun. 2022, doi: 10.3389/fenvs.2022.880246.

[3] A. P. Periyasamy, “Recent Advances in the Remediation of Textile-Dye-Containing Wastewater: Prioritizing Human Health and Sustainable Wastewater Treatment,” *Sustainability*, vol. 16, no. 2, Art. no. 2, Jan. 2024, doi: 10.3390/su16020495.

[4] S. Dong *et al.*, “Recent developments in heterogeneous photocatalytic water treatment using visible light-responsive photocatalysts: a review,” *RSC Adv.*, vol. 5, no. 19, pp. 14610–14630, Jan. 2015, doi: 10.1039/C4RA13734E.

[5] “Materials | Free Full-Text | Carbon-Based Nanocomposites as Fenton-Like Catalysts in Wastewater Treatment Applications: A Review.” Accessed: Jun. 13, 2024. [Online]. Available: https://www.mdpi.com/1996-1944/14/10/2643

[6] Y. Luo *et al.*, “g-C3N4-based photocatalysts for organic pollutant removal: a critical review,” *Carbon Res.*, vol. 2, no. 1, p. 14, Apr. 2023, doi: 10.1007/s44246-023-00045-5.

[7] P. V. D. Voort, K. Leus, and E. D. Canck, *Introduction to Porous Materials*. John Wiley & Sons, 2019.

[8] “Journal of Porous Materials,” SpringerLink. Accessed: Jun. 08, 2024. [Online]. Available: https://link.springer.com/journal/10934

[9] V. Solano-Umaña and J. R. Vega-Baudrit, “Micro, Meso and Macro Porous Materials on Medicine,” *J. Biomater. Nanobiotechnology*, vol. 6, no. 4, Art. no. 4, Sep. 2015, doi: 10.4236/jbnb.2015.64023.

[10] U. G. T. M. Sampath, Y. C. Ching, C. H. Chuah, J. J. Sabariah, and P.-C. Lin, “Fabrication of Porous Materials from Natural/Synthetic Biopolymers and Their Composites,” *Materials*, vol. 9, no. 12, p. 991, Dec. 2016, doi: 10.3390/ma9120991.

[11] “Porous materials for environmental applications | LE STUDIUM.” Accessed: Jun. 08, 2024. [Online]. Available: https://www.lestudium-ias.com/content/porous-materials-environmental-applications

[12] R. Luque *et al.*, “Functionalized interconnected porous materials for heterogeneous catalysis, energy conversion and storage applications: Recent advances and future perspectives,” *Mater. Today*, vol. 73, pp. 105–129, Mar. 2024, doi: 10.1016/j.mattod.2023.05.001.

[13] A. Garg, S. Laha, M. Eswaramoorthy, and T. K. Maji, “Porous Materials for Sustainable Energy Applications: Promises and Challenges,” in *Energy Materials*, WORLD SCIENTIFIC, 2022, pp. 249–286. doi: 10.1142/9789811270956_0009.

[14] M. Usman *et al.*, “A review of metal-organic frameworks/graphitic carbon nitride composites for solar-driven green H2 production, CO2 reduction, and water purification,” *J. Environ. Chem. Eng.*, vol. 10, p. 107548, Mar. 2022, doi: 10.1016/j.jece.2022.107548.

[15] A. Jose, T. Mathew, N. Fernández-Navas, and C. J. Querebillo, “Porous Inorganic Nanomaterials: Their Evolution towards Hierarchical Porous Nanostructures,” *Micro*, vol. 4, no. 2, Art. no. 2, Jun. 2024, doi: 10.3390/micro4020016.

[16] H. Wang, L. Wang, and F.-S. Xiao, “Metal@Zeolite Hybrid Materials for Catalysis,” *ACS Cent. Sci.*, vol. 6, no. 10, pp. 1685–1697, Oct. 2020, doi: 10.1021/acscentsci.0c01130.

[17] W. Zhang *et al.*, “Regulation of Porosity in MOFs: A Review on Tunable Scaffolds and Related Effects and Advances in Different Applications,” *J. Environ. Chem. Eng.*, vol. 10, no. 6, p. 108836, Dec. 2022, doi: 10.1016/j.jece.2022.108836.

[18] L. Feng, K.-Y. Wang, X.-L. Lv, T.-H. Yan, and H.-C. Zhou, “Hierarchically porous metal–organic frameworks: synthetic strategies and applications,” *Natl. Sci. Rev.*, vol. 7, no. 11, pp. 1743–1758, Nov. 2019, doi: 10.1093/nsr/nwz170.

[19] M. Fakoor and S. M. J. Tabatabaee, “Investigation into effective mechanical properties of porous material produced by the additive manufacturing method,” *Frat. Ed Integrità Strutt.*, vol. 17, no. 65, Art. no. 65, Jun. 2023, doi: 10.3221/IGF-ESIS.65.14.

[20] H. NAKAJIMA, “Fabrication, properties, and applications of porous metals with directional pores,” *Proc. Jpn. Acad. Ser. B Phys. Biol. Sci.*, vol. 86, no. 9, pp. 884–899, Nov. 2010, doi: 10.2183/pjab.86.884.

[21] L. H. K. Alfhaid, “Recent advance in functionalized mesoporous silica nanoparticles with stimuli-responsive polymer brush for controlled drug delivery,” *Soft Mater.*, vol. 20, no. 3, pp. 364–378, Jul. 2022, doi: 10.1080/1539445X.2022.2028831.

[22] T. P. Lodge and P. C. Hiemenz, *Polymer Chemistry*, 3rd ed. Boca Raton: CRC Press, 2020. doi: 10.1201/9780429190810.

[23] S. Thomas, P. M. Visakh, and Aji. P. Mathew, Eds., *Advances in Natural Polymers: Composites and Nanocomposites*, vol. 18. in Advanced Structured Materials, vol. 18. Berlin, Heidelberg: Springer, 2013. doi: 10.1007/978-3-642-20940-6.

[24] O. I. Parisi, M. Curcio, and F. Puoci, “Polymer Chemistry and Synthetic Polymers,” in *Advanced Polymers in Medicine*, F. Puoci, Ed., Cham: Springer International Publishing, 2015, pp. 1–31. doi: 10.1007/978-3-319-12478-0_1.

[25] X. Zhu *et al.*, “Design of polymer-based nanoreactors for efficient acid/base cascade catalysis: A comparative study of site isolation strategies,” *J. Mol. Struct.*, vol. 1285, p. 135482, Aug. 2023, doi: 10.1016/j.molstruc.2023.135482.

[26] *Handbook of Polymers*. 2016. Accessed: Jun. 12, 2024. [Online]. Available: https://shop.elsevier.com/books/handbook-of-polymers/wypych/978-1-895198-92-8

[27] S. Kumari *et al.*, “Synthetic and catalytic perspectives of polystyrene supported metal catalyst,” *J. Iran. Chem. Soc.*, vol. 21, no. 4, pp. 951–1010, Apr. 2024, doi: 10.1007/s13738-024-02970-7.

[28] “Polyaniline-based nanocomposites for electromagnetic interference shielding applications: A review - Muhammad Zahid, Rukhsar Anum, Sabahat Siddique, HM Fayzan

Shakir, ZA Rehan, 2023.” Accessed: Jun. 12, 2024. [Online]. Available: https://journals.sagepub.com/doi/10.1177/08927057211022408

[29] “(PDF) Matrix and Reinforcement Materials for Metal Matrix Composites.” Accessed: Jun. 12, 2024. [Online]. Available: https://www.researchgate.net/publication/339593350_Matrix_and_Reinforcement_Materials_for_Metal_Matrix_Composites

[30] J. Selvam, I. Dinaharan, and R. Rai, “Matrix and Reinforcement Materials for Metal Matrix Composites,” in *Reference Module in Materials Science and Materials Engineering*, 2020. doi: 10.1016/B978-0-12-803581-8.11890-9.

[31] R. R. Naslain and M. Pomeroy, “Ceramic Matrix Composites: Matrices and Processing,” in *Reference Module in Materials Science and Materials Engineering*, Elsevier, 2016. doi: 10.1016/B978-0-12-803581-8.02317-1.

[32] D. K. Rajak, D. D. Pagar, R. Kumar, and C. I. Pruncu, “Recent progress of reinforcement materials: a comprehensive overview of composite materials,” *J. Mater. Res. Technol.*, vol. 8, no. 6, pp. 6354–6374, Nov. 2019, doi: 10.1016/j.jmrt.2019.09.068.

[33] “Polymer Matrix Composite - an overview | ScienceDirect Topics.” Accessed: Jun. 12, 2024. [Online]. Available: https://www.sciencedirect.com/topics/materials-science/polymer-matrix-composite

[34] E. G. S. Hashem, “12.35 - Study of the mechanical properties of the metal matrix composites developed with alumina particles,” in *Comprehensive Materials Processing (Second Edition)*, S. Hashmi, Ed., Oxford: Elsevier, 2024, pp. 472–484. doi: 10.1016/B978-0-323-96020-5.00037-6.

[35] S. Shrivastava, D. K. Rajak, T. Joshi, D. K. Singh, and D. P. Mondal, “Ceramic Matrix Composites: Classifications, Manufacturing, Properties, and Applications,” *Ceramics*, vol. 7, no. 2, Art. no. 2, Jun. 2024, doi: 10.3390/ceramics7020043.

[36] P. H. C. Camargo, K. G. Satyanarayana, and F. Wypych, “Nanocomposites: synthesis, structure, properties and new application opportunities,” *Mater. Res.*, vol. 12, pp. 1–39, Mar. 2009, doi: 10.1590/S1516-14392009000100002.

[37] “(PDF) NANOCOMPOSITES MATERIALS DEFINITIONS, TYPES AND SOME OF THEIR APPLICATIONS: A REVIEW.” Accessed: Jun. 12, 2024. [Online]. Available: https://www.researchgate.net/publication/360823018_NANOCOMPOSITES_MATERIALS_DEFINITIONS_TYPES_AND_SOME_OF_THEIR_APPLICATIONS_A_REVIEW

[38] R. S. M. Almeida, H. Farhandi, K. Tushtev, and K. Rezwan, “Enhancing thermal stability of oxide ceramic matrix composites via matrix doping,” *J. Eur. Ceram. Soc.*, vol. 42, no. 7, pp. 3282–3289, Jul. 2022, doi: 10.1016/j.jeurceramsoc.2022.02.040.

[39] “(PDF) Polymer matrix nanocomposites from the ecological aspect in the automotive industry.” Accessed: Jun. 12, 2024. [Online]. Available: https://www.researchgate.net/publication/378747389_Polymer_matrix_nanocomposites_from_the_ecological_aspect_in_the_automotive_industry

[40] F. Ali *et al.*, “PANI-based nanocomposites synthetic methods, properties, and catalytic applications,” *Inorg. Chem. Commun.*, vol. 161, p. 112077, Mar. 2024, doi: 10.1016/j.inoche.2024.112077.

[41] A. M. Díez-Pascual, “Carbon-Based Polymer Nanocomposites for High-Performance Applications,” *Polymers*, vol. 12, no. 4, p. 872, Apr. 2020, doi: 10.3390/polym12040872.

[42] P. A. Bolla, S. Huggias, M. A. Serradell, J. F. Ruggera, and M. L. Casella, “Synthesis and Catalytic Application of Silver Nanoparticles Supported on Lactobacillus kefiri S-Layer Proteins,” *Nanomaterials*, vol. 10, no. 11, p. 2322, Nov. 2020, doi: 10.3390/nano10112322.

[43] G. Liao, J. Fang, Q. Li, S. Li, Z. Xu, and B. Fang, “Ag-based Nanocomposites: Synthesis and Applications in Catalysis,” *Nanoscale*, vol. 11, Mar. 2019, doi: 10.1039/C9NR01408J.

[44] A. Selim, S. Kaur, A. H. Dar, S. Sartaliya, and G. Jayamurugan, “Synergistic Effects of Carbon Dots and Palladium Nanoparticles Enhance the Sonocatalytic Performance for Rhodamine B Degradation in the Absence of Light,” *ACS Omega*, vol. 5, no. 35, pp. 22603–22613, Aug. 2020, doi: 10.1021/acsomega.0c03312.

[45] M. B. Askari, S. Azizi, M. T. T. Moghadam, M. Seifi, S. M. Rozati, and A. Di Bartolomeo, “MnCo2O4/NiCo2O4/rGO as a Catalyst Based on Binary Transition Metal Oxide for the Methanol Oxidation Reaction,” *Nanomaterials*, vol. 12, no. 22, Art. no. 22, Jan. 2022, doi: 10.3390/nano12224072.

[46] M. B. Askari, H. Beitollahi, and A. Di Bartolomeo, “Methanol and Ethanol Electrooxidation on ZrO2/NiO/rGO,” *Nanomaterials*, vol. 13, no. 4, p. 679, Feb. 2023, doi: 10.3390/nano13040679.

[47] A. Zadehnazari, “Metal oxide/polymer nanocomposites: A review on recent advances in fabrication and applications,” *Polym.-Plast. Technol. Mater.*, vol. 62, pp. 655–700, Oct. 2022, doi: 10.1080/25740881.2022.2129387.

[48] B. Martínez-Navarro, R. Sanchis, E. Asedegbega-Nieto, B. Solsona, and F. Ivars-Barceló, “(Ag)Pd-Fe3O4 Nanocomposites as Novel Catalysts for Methane Partial Oxidation at Low Temperature,” *Nanomaterials*, vol. 10, no. 5, p. 988, May 2020, doi: 10.3390/nano10050988.

[49] P. P. Singh and V. Srivastava, “Recent advances in visible-light graphitic carbon nitride (g-C3N4) photocatalysts for chemical transformations,” *RSC Adv.*, vol. 12, no. 28, pp. 18245–18265, doi: 10.1039/d2ra01797k.

[50] “LBL Scientists Awarded Patent on Superhard Material.” Accessed: Jun. 12, 2024. [Online]. Available: https://www2.lbl.gov/Science-Articles/Archive/superhard-materials.html

[51] Y. Ezhumalai, P. Kumaresan, T. Jayapalan, Y. Ezhumalai, P. Kumaresan, and T. Jayapalan, “Graphite Carbon Nitride,” in *Photocatalysts - New Perspectives*, IntechOpen, 2022. doi: 10.5772/intechopen.104976.

[52] “Graphene for batteries, supercapacitors and beyond | Nature Reviews Materials.” Accessed: Jun. 12, 2024. [Online]. Available: https://www.nature.com/articles/natrevmats201633

[53] D. Teter and R. Hemley, “Low-Compressibility Carbon Nitrides,” *Science*, vol. 271, pp. 53–55, Jan. 1996, doi: 10.1126/science.271.5245.53.

[54] F. M. Yap, G. Z. S. Ling, B. J. Su, J. Y. Loh, and W.-J. Ong, “Recent advances in structural modification on graphitic carbon nitride (g-C_3N_4)-based photocatalysts for high-efficiency photocatalytic H_2O_2 production,” *Nano Res. Energy*, vol. 3, no. 1, Mar. 2024, doi: 10.26599/NRE.2023.9120091.

[55] J. Pei, H. Li, S. Zhuang, D. Zhang, and D. Yu, “Recent Advances in g-C3N4 Photocatalysts: A Review of Reaction Parameters, Structure Design and Exfoliation Methods,” *Catalysts*, vol. 13, no. 11, Art. no. 11, Nov. 2023, doi: 10.3390/catal13111402.

[56] Q. Wang *et al.*, “Recent Advances in g-C3N4-Based Materials and Their Application in Energy and Environmental Sustainability,” *Molecules*, vol. 28, p. 432, Jan. 2023, doi: 10.3390/molecules28010432.

[57] A. Alaghmandfard and K. Ghandi, “A Comprehensive Review of Graphitic Carbon Nitride (g-C3N4)–Metal Oxide-Based Nanocomposites: Potential for Photocatalysis and Sensing,” *Nanomaterials*, vol. 12, no. 2, p. 294, Jan. 2022, doi: 10.3390/nano12020294.

[58] M. Pourmadadi *et al.*, “Two-Dimensional Graphitic Carbon Nitride (g-C3N4) Nanosheets and Their Derivatives for Diagnosis and Detection Applications,” *J. Funct. Biomater.*, vol. 13, no. 4, Art. no. 4, Dec. 2022, doi: 10.3390/jfb13040204.

[59] D. Bhanderi, P. Lakhani, and C. Modi, “Graphitic carbon nitride (g-C3N4) as an emerging photocatalyst for sustainable environmental applications: a comprehensive review,” *RSC Sustain.*, vol. 2, Dec. 2023, doi: 10.1039/d3su00382e.

[60] A. Schwarzer, T. Saplinova, and E. Kroke, “Tri-s-triazines (s-heptazines)—From a ‘mystery molecule’ to industrially relevant carbon nitride materials,” *Coord. Chem. Rev.*, vol. 257, pp. 2032–2062, Jan. 2013, doi: 10.1016/j.ccr.2012.12.00.

[61] D. Bhanderi, P. Lakhani, and C. K. Modi, “Graphitic carbon nitride (g-C3N4) as an emerging photocatalyst for sustainable environmental applications: a comprehensive review,” *RSC Sustain.*, vol. 2, no. 2, pp. 265–287, Feb. 2024, doi: 10.1039/D3SU00382E.

[62] “Fig. 2. Structure of Triazine (a) [21] and tri-s-triazine (b) in g-C 3...,” ResearchGate. Accessed: Jun. 12, 2024. [Online]. Available: https://www.researchgate.net/figure/Structure-of-Triazine-a-21-and-tri-s-triazine-b-in-g-C-3-N-4-28_fig1_366860083

[63] Q. Li *et al.*, “Preparation of g-C3N4/TCNQ Composite and Photocatalytic Degradation of Pefloxacin,” *Micromachines*, vol. 14, no. 5, p. 941, Apr. 2023, doi: 10.3390/mi14050941.

[64] J. Pei, H. Li, S. Zhuang, D. Zhang, and D. Yu, “Recent Advances in g-C3N4 Photocatalysts: A Review of Reaction Parameters, Structure Design and Exfoliation Methods,” *Catalysts*, vol. 13, no. 11, Art. no. 11, Nov. 2023, doi: 10.3390/catal13111402.

[65] Q. Wang *et al.*, “Recent Advances in g-C3N4-Based Materials and Their Application in Energy and Environmental Sustainability,” *Molecules*, vol. 28, no. 1, p. 432, Jan. 2023, doi: 10.3390/molecules28010432.

[66] J. Zhu, P. Xiao, H. Li, and S. A. C. Carabineiro, “Graphitic Carbon Nitride: Synthesis, Properties, and Applications in Catalysis,” *ACS Appl. Mater. Interfaces*, vol. 6, no. 19, pp. 16449–16465, Oct. 2014, doi: 10.1021/am502925j.

[67] S. Ye, R. Wang, M.-Z. Wu, and Y.-P. Yuan, “A review on g-C3N4 for photocatalytic water splitting and CO2 reduction,” *Appl. Surf. Sci.*, vol. 358, Aug. 2015, doi: 10.1016/j.apsusc.2015.08.173.

[68] Q. Li, Y. He, and R. Peng, “Graphitic carbon nitride (g-C3N4) as a metal-free catalyst for thermal decomposition of ammonium perchlorate,” *RSC Adv.*, vol. 5, no. 31, pp. 24507–24512, Mar. 2015, doi: 10.1039/C5RA01157D.

[69] R.-H. Gao, Q. Ge, N. Jiang, H. Cong, M. Liu, and Y.-Q. Zhang, “Graphitic carbon nitride (g-C3N4)-based photocatalytic materials for hydrogen evolution,” *Front. Chem.*, vol. 10, Oct. 2022, doi: 10.3389/fchem.2022.1048504.

[70] M. Sajid, Z. A. Chandio, B. Hwang, T. G. Yun, and J. Y. Cheong, “Graphitic carbon nitrides as electrode supporting materials for lithium-ion batteries: what lies ahead in view of the current challenges?” *Front. Energy Res.*, vol. 11, Dec. 2023, doi: 10.3389/fenrg.2023.1285044.

[71] V. S. Bhati, V. Takhar, R. Raliya, M. Kumar, and R. Banerjee, “Recent advances in g-C3N4 based gas sensors for the detection of toxic and flammable gases: a review,” *Nano Express*, vol. 3, no. 1, p. 014003, Mar. 2022, doi: 10.1088/2632-959X/ac477b.

[72] A. Alaghmandfard and K. Ghandi, “A Comprehensive Review of Graphitic Carbon Nitride (g-C3N4)–Metal Oxide-Based Nanocomposites: Potential for Photocatalysis and Sensing,” *Nanomaterials*, vol. 12, no. 2, p. 294, Jan. 2022, doi: 10.3390/nano12020294.

[73] A. Wang, C. Wang, L. Fu, W. Wong-Ng, and Y. Lan, “Recent Advances of Graphitic Carbon Nitride-Based Structures and Applications in Catalyst, Sensing, Imaging, and LEDs,” *Nano-Micro Lett.*, vol. 9, no. 4, p. 47, Jun. 2017, doi: 10.1007/s40820-017-0148-2.

[74] L. Hammoud, C. Marchal, V. Caps, J. Toufaily, T. Hamieh, and V. Keller, “Influence of low level of non-metal doping on g-C3N4 performance for H2 production from water under solar light irradiation,” *Int. J. Hydrog. Energy*, 2023, doi: 10.1016/j.ijhydene.2023.03.284.

[75] D. Piyachatpanom and S. Watcharamaisakul, “SYNTHESIS OF GRAPHITIC CARBON NITRIDE (g-C3N4) POWDER FROM MELAMINE BY PYROLYSIS PROCESS,” vol. 28, no. 2, 2021.

[76] L. Wang *et al.*, “One-step, high-yield synthesis of g-C3N4 nanosheets for enhanced visible light photocatalytic activity,” *RSC Adv.*, vol. 9, no. 67, pp. 39304–39314, doi: 10.1039/c9ra08922e.

[77] N. Haneklaus, “Calcination,” in *Reference Module in Earth Systems and Environmental Sciences*, 2021. doi: 10.1016/B978-0-12-819725-7.00161-6.

[78] K. Li *et al.*, “Synthesis of g-C3N4 Derived from Different Precursors for Photodegradation of Sulfamethazine under Visible Light,” *Processes*, vol. 11, no. 2, Art. no. 2, Feb. 2023, doi: 10.3390/pr11020528.

[79] R. Liu *et al.*, “Ag-Modified g-C3N4 Prepared by a One-Step Calcination Method for Enhanced Catalytic Efficiency and Stability,” *ACS Omega*, vol. 5, no. 31, pp. 19615–19624, Jul. 2020, doi: 10.1021/acsomega.0c02161.

[80] S. Iravani, H. Korbekandi, S. V. Mirmohammadi, and B. Zolfaghari, “Synthesis of silver nanoparticles: chemical, physical and biological methods,” *Res. Pharm. Sci.*, vol. 9, no. 6, pp. 385–406, 2014.

[81] X. Li, W. Yang, J. Deng, and Y. Lin, “Surface plasmon resonance effects of silver nanoparticles in graphene-based dye-sensitized solar cells,” *Front. Mater.*, vol. 10, May 2023, doi: 10.3389/fmats.2023.1137771.

[82] “Silver nanoparticles embedded 2D g-C3N4 nanosheets toward excellent photocatalytic hydrogen evolution under visible light - IOPscience.” Accessed: Jun. 13, 2024. [Online]. Available: https://iopscience.iop.org/article/10.1088/1361-6528/ac493d/meta

[83] B. P. Colman *et al.*, “Low Concentrations of Silver Nanoparticles in Biosolids Cause Adverse Ecosystem Responses under Realistic Field Scenario,” *PLoS ONE*, vol. 8, no. 2, p. e57189, Feb. 2013, doi: 10.1371/journal.pone.0057189.

[84] F. P. Mehr, M. Khanjani, and P. Vatani, “Synthesis of Nano-Ag particles using sodium borohydride,” *Orient. J. Chem.*, vol. 31, no. 3, pp. 1831–1833, Sep. 2015.

[85] F. P. Mehr, M. Khanjani, and P. Vatani, “Synthesis of Nano-Ag particles using sodium borohydride,” *Orient. J. Chem.*, vol. 31, no. 3, pp. 1831–1833, Sep. 2015.

[86] R. Liu *et al.*, “Ag-Modified g-C3N4 Prepared by a One-Step Calcination Method for Enhanced Catalytic Efficiency and Stability,” *ACS Omega*, vol. 5, no. 31, pp. 19615–19624, Jul. 2020, doi: 10.1021/acsomega.0c02161.

[87] J. Hou *et al.*, “Synthesis of Silver Nanoparticles-Modified Graphitic Carbon Nitride Nanosheets for Highly Efficient Photocatalytic Hydrogen Peroxide Evolution,” *Molecules*, vol. 27, no. 17, p. 5535, Aug. 2022, doi: 10.3390/molecules27175535.

[88] “Nanomaterials | Free Full-Text | Photocatalytic Activity of Ag Nanoparticles Deposited on Thermoexfoliated g-C3N4.” Accessed: Jun. 13, 2024. [Online]. Available: https://www.mdpi.com/2079-4991/14/7/623

[89] H. Jabeen *et al.*, “Advances in modifications of Ag/g-C 3 N 4 for stable and effective photoanode for OER,” Nov. 2023, doi: 10.1016/j.optmat.2023.114376.

[90] E. K. Orcutt, S. J. Varapragasam, Z. C. Peterson, J. M. Andriolo, J. L. Skinner, and E. M. Grumstrup, “Ultrafast Charge Injection in Silver-Modified Graphitic Carbon Nitride,” *ACS Appl. Mater. Interfaces*, vol. 15, no. 12, pp. 15478–15485, Mar. 2023, doi: 10.1021/acsami.2c22870.

[91] C. M. Friend and B. Xu, “Heterogeneous Catalysis: A Central Science for a Sustainable Future,” *Acc. Chem. Res.*, vol. 50, no. 3, pp. 517–521, Mar. 2017, doi: 10.1021/acs.accounts.6b00510.

[92] “Heterogeneous Catalysis - Schlögl - 2015 - Angewandte Chemie International Edition - Wiley Online Library.” Accessed: Jun. 13, 2024. [Online]. Available: https://onlinelibrary.wiley.com/doi/10.1002/anie.201410738

[93] C. Vogt and B. M. Weckhuysen, “The concept of active site in heterogeneous catalysis,” *Nat. Rev. Chem.*, vol. 6, no. 2, pp. 89–111, Feb. 2022, doi: 10.1038/s41570-021-00340-y.

[94] S. P *et al.*, “Graphitic carbon nitride (g-C3N4) based heterogeneous single atom catalysts: synthesis, characterisation and catalytic applications,” *J. Mater. Chem. A*, vol. 11, no. 16, pp. 8599–8646, Apr. 2023, doi: 10.1039/D2TA09776A.

[95] J. Dong, Y. Zhang, M. I. Hussain, W. Zhou, Y. Chen, and L.-N. Wang, “g-C3N4: Properties, Pore Modifications, and Photocatalytic Applications,” *Nanomaterials*, vol. 12, no. 1, p. 121, Dec. 2021, doi: 10.3390/nano12010121.

[96] M. Hu, Y. Liu, Z. Yao, L. Ma, and X. Wang, “Catalytic reduction for water treatment,” *Front. Environ. Sci. Eng.*, vol. 12, no. 1, Art. no. 1, Feb. 2018, doi: 10.1007/s11783-017-0972-0.

[97] J. Liu and J. Gao, “Catalytic reduction of water pollutants: knowledge gaps, lessons learned, and new opportunities,” *Front. Environ. Sci. Eng.*, vol. 17, no. 2, p. 26, Nov. 2022, doi: 10.1007/s11783-023-1626-z.

[98] F. Gao *et al.*, “A Review on Selective Catalytic Reduction of NOx by NH3 over Mn–Based Catalysts at Low Temperatures: Catalysts, Mechanisms, Kinetics and DFT Calculations,” *Catalysts*, vol. 7, no. 7, Art. no. 7, Jul. 2017, doi: 10.3390/catal7070199.

[99] C. Feng, X. Liu, T. Zhu, and M. Tian, “Catalytic oxidation of CO on noble metal-based catalysts,” *Environ. Sci. Pollut. Res. Int.*, vol. 28, no. 20, pp. 24847–24871, May 2021, doi: 10.1007/s11356-021-13008-3.

[100] C. N. C. Hitam, A. A. Jalil, and S. Triwahyono, “Synthesis of Zinc Oxide Supported on Titanium Dioxide for Photocatalytic Oxidative Desulfurization of Dibenzothiophene,” *J. Energy Saf. Technol. JEST*, vol. 1, no. 1, Art. no. 1, Aug. 2018, doi: 10.11113/jest.v1n1.2.

[101] Murugan Arunachalapandi and Selvaraj Mohana Roopan, “Environment Friendly g-C3N4-Based Catalysts and Their Recent Strategy in Organic Transformations,” *High Energy Chem.*, vol. 56, no. 2, pp. 73–90, Apr. 2022, doi: 10.1134/S0018143922020102.

[102] F. Benali *et al.*, “Catalytic Reduction of Dyes and Antibacterial Activity of AgNPs@Zn@Alginate Composite Aerogel Beads,” *Polymers*, vol. 14, no. 22, Art. no. 22, Jan. 2022, doi: 10.3390/polym14224829.

[103] I. Khan *et al.*, “Review on Methylene Blue: Its Properties, Uses, Toxicity and Photodegradation,” *Water*, vol. 14, no. 2, p. 242, Jan. 2022, doi: 10.3390/w14020242.

[104] PubChem, “Methylene Blue.” Accessed: Jun. 13, 2024. [Online]. Available: https://pubchem.ncbi.nlm.nih.gov/compound/6099

[105] N. Isa and Z. Lockman, “Methylene blue dye removal on silver nanoparticles reduced by Kyllinga brevifolia,” *Environ. Sci. Pollut. Res. Int.*, vol. 26, no. 11, pp. 11482–11495, Apr. 2019, doi: 10.1007/s11356-019-04583-7.

[106] X. Jaramillo-Fierro and G. Cuenca, “Enhancing Methylene Blue Removal through Adsorption and Photocatalysis—A Study on the GO/ZnTiO3/TiO2 Composite,” *Int. J. Mol. Sci.*, vol. 25, no. 8, Art. no. 8, Jan. 2024, doi: 10.3390/ijms25084367.

[107] Z. G. Asmare, B. A. Aragaw, M. Atlabachew, and T. A. Wubieneh, “Kaolin-Supported Silver Nanoparticles as an Effective Catalyst for the Removal of Methylene Blue Dye from Aqueous Solutions,” *ACS Omega*, vol. 8, no. 1, pp. 480–491, Jan. 2023, doi: 10.1021/acsomega.2c05265.

[108] “Chemical reduction of methylene blue in the presence of nanocatalysts: a critical review.” Accessed: Jun. 13, 2024. [Online]. Available: https://www.degruyter.com/document/doi/10.1515/revce-2018-0047/html?lang=en

[109] N. S. Alkayal, M. Ibrahim, N. Tashkandi, and M. M. Alotaibi, “Efficient Reduction in Methylene Blue Using Palladium Nanoparticles Supported by Melamine-Based Polymer,” *Materials*, vol. 16, no. 17, p. 5887, Aug. 2023, doi: 10.3390/ma16175887.

[110] Y.-N. Liu *et al.*, “Hydrogenation/oxidation induced efficient reversible color switching between methylene blue and leuco-methylene blue,” *RSC Adv.*, vol. 7, no. 48, pp. 30080–30085, 2017, doi: 10.1039/C7RA04498D.

[111] S. Benkhaya, S. M’rabet, and A. El Harfi, “Classifications, properties, recent synthesis and applications of azo dyes,” *Heliyon*, vol. 6, no. 1, p. e03271, Jan. 2020, doi: 10.1016/j.heliyon. 2020.e03271.

[112] PubChem, “Methyl orange.” Accessed: Jun. 13, 2024. [Online]. Available: https://pubchem.ncbi.nlm.nih.gov/compound/23673835

[113] P. Peerakiatkhajohn, T. Butburee, J.-H. Sul, S. Thaweesak, and J.-H. Yun, “Efficient and Rapid Photocatalytic Degradation of Methyl Orange Dye Using Al/ZnO Nanoparticles,” *Nanomaterials*, vol. 11, no. 4, Art. no. 4, Apr. 2021, doi: 10.3390/nano11041059.

[114] Y. Shi, Z. Yang, L. Xing, X. Zhang, X. Li, and D. Zhang, “Recent advances in the biodegradation of azo dyes,” *World J. Microbiol. Biotechnol.*, vol. 37, no. 8, p. 137, Jul. 2021, doi: 10.1007/s11274-021-03110-6.

[115] E. Meydan, S. Demirci, N. Aktas, N. Sahiner, and O. F. Ozturk, “Catalytic performance of boron-containing magnetic metal nanoparticles in methylene blue degradation reaction and mixture with other pollutants,” *Inorg. Chem. Commun.*, vol. 126, p. 108474, Apr. 2021, doi: 10.1016/j.inoche.2021.108474.

[116] T. H. V. Luong, T. H. T. Nguyen, B. V. Nguyen, N. K. Nguyen, T. Q. C. Nguyen, and G. H. Dang, “Efficient degradation of methyl orange and methylene blue in aqueous solution

using a novel Fenton-like catalyst of CuCo-ZIFs," *Green Process. Synth.*, vol. 11, no. 1, pp. 71–83, Jan. 2022, doi: 10.1515/gps-2022-0006.

[117] S. Elgharbi, A. Boubakri, S. Bouguecha, H. Bilel, S. I. Matalka, and A. Hafiane, "Membrane Distillation for Methylene Blue Dye Removal from Wastewater: Investigating Process Optimization and Membrane Wettability," *Arab. J. Sci. Eng.*, vol. 49, no. 6, pp. 8131–8145, Jun. 2024, doi: 10.1007/s13369-024-08756-6.

[118] H. Saeed *et al.*, "Efficient dye degradation in the presence of reducing agent and bactericidal behavior with in silico molecular docking of z-scheme P3HT/g-C3N4 doped CuO heterojunction," *Surf. Interfaces*, vol. 38, p. 102804, Jun. 2023, doi: 10.1016/j.surfin.2023.102804.

[119] A. S. Najm, N. Ahmad Ludin, I. Jaber, N. H. Hamid, and H. Salah Naeem, "Influence of the concentration of chenodeoxycholic acid on the performance of the N719 dye," *Inorganica Chim. Acta*, vol. 533, p. 120776, Apr. 2022, doi: 10.1016/j.ica.2021.120776.

[120] K. Tian, F. Shi, M. Cao, Q. Zheng, and G. Zhang, "A Review of Persulfate Activation by Magnetic Catalysts to Degrade Organic Contaminants: Mechanisms and Applications," *Catalysts*, vol. 12, no. 9, Art. no. 9, Sep. 2022, doi: 10.3390/catal12091058.

[121] "Photocatalytic degradation of organic dye under UV light using CaCu3Ti4O12 nanoparticles synthesized by sol gel route: Effect of calcination temperature | Semantic Scholar." Accessed: Jun. 13, 2024. [Online]. Available: https://www.semanticscholar.org/paper/Photocatalytic-degradation-of-organic-dye-under-UV-Ling-Iqbal/9481c34320972a2327142d3ef76f56bc0fc11832

[122] S. Kalidhasan, D.-G. Park, K. S. Jin, and H.-Y. Lee, "Engineered polymer–clay–copper oxides catalyst for the oxidation and reduction of organic molecules: synergy of degradation and instinctive interface stability by polymer self-healing function," *Surf. Interfaces*, vol. 39, p. 102934, Jul. 2023, doi: 10.1016/j.surfin.2023.102934.

[123] "X-ray Diffraction," in *Practical Guide to Materials Characterization*, John Wiley & Sons, Ltd, 2022, pp. 15–42. doi: 10.1002/9783527838820.ch2.

[124] A. Nandiyanto, R. Ragadhita, M. Fiandini, and I. Ijost, "Interpretation of Fourier Transform Infrared Spectra (FTIR): A Practical Approach in the Polymer/Plastic Thermal Decomposition," *Indones. J. Sci. Technol.*, vol. 8, pp. 113–126, Apr. 2023, doi: 10.17509/ijost. v8i1.53297.

[125] K. Cole and B. S. Levine, "Ultraviolet-Visible Spectrophotometry," in *Principles of Forensic Toxicology*, B. S. Levine and S. KERRIGAN, Eds., Cham: Springer International Publishing, 2020, pp. 127–134. doi: 10.1007/978-3-030-42917-1_10.

[126] "Synergistic effect of ZnO/Ag2O@g-C3N4 based nanocomposites embedded in carrageenan matrix for dye degradation in water: Heliyon." Accessed: Jun. 13, 2024. [Online]. Available: https://www.cell.com/heliyon/fulltext/S2405-8440(24)07140-8?_returnURL=https%3A%2F%2Flinkinghub.elsevier.com%2Fretrieve%2Fpii%2FS2405844024071408%3Fshowall%3Dtrue

[127] B. Gauri, K. Vidya, S. Gadale -Dagade, and S. Waghmode, “Synthesis and Characterization of Ag/AgO nanoparticles as alcohol sensor,” vol. 20, Oct. 2016.

[128] B. Asli *et al.*, “Catalytic Reduction and Antibacterial Activity of MCM-41 Modified by Silver Nanoparticles,” *Silicon*, vol. 14, no. 18, pp. 12587–12598, Dec. 2022, doi: 10.1007/s12633-022-01963-6.

[129] “FT-IR Characterization Lecture note.pdf,” SlideShare. Accessed: Jun. 13, 2024. [Online]. Available: https://www.slideshare.net/slideshow/ftir-characterization-lecture-notepdf/266306533

[130] M. Hachemaoui *et al.*, “Composites beads based on Fe3O4@MCM-41 and calcium alginate for enhanced catalytic reduction of organic dyes,” *Int. J. Biol. Macromol.*, vol. 164, pp. 468–479, Dec. 2020, doi: 10.1016/j.ijbiomac.2020.07.128.

[131] “Preparation of silver-nanoparticle-loaded magnetic biochar/poly(dopamine) composite as catalyst for reduction of organic dyes. | Semantic Scholar.” Accessed: Jun. 13, 2024. [Online]. Available: https://www.semanticscholar.org/paper/Preparation-of-silver-nanoparticle-loaded-magnetic-Li-Jiang/4659833d5e0d960e03f5d24704e191303623dc60

[132] “In situ synthesis of silver nanostructures on magnetic Fe3O4@C core–shell nanocomposites and their application in catalytic reduction reactions | Semantic Scholar.” Accessed: Jun. 13, 2024. [Online]. Available: https://www.semanticscholar.org/paper/In-situ-synthesis-of-silver-nanostructures-on-and-Zhu-Wang/d77accf109031c3784dee06146d8e0a7d3405608

[133] D. Nagarajan and S. Venkatanarasimhan, “Copper (II) oxide nanoparticles coated cellulose sponge—an effective heterogeneous catalyst for the reduction of toxic organic dyes,” *Environ. Sci. Pollut. Res.*, vol. 26, no. 22, pp. 22958–22970, Aug. 2019, doi: 10.1007/s11356-019-05419-0.

[134] “Highly efficient catalytic reductive degradation of various organic dyes by Au/CeO 2 -TiO 2 nano-hybrid | Journal of Chemical Sciences.” Accessed: Jun. 13, 2024. [Online]. Available: https://link.springer.com/article/10.1007/s12039-016-1203-0

[135] “Preparation of Cu nanoparticle loaded SBA-15 and their excellent catalytic activity in reduction of variety of dyes - ScienceDirect.” Accessed: Jun. 13, 2024. [Online]. Available: https://www.sciencedirect.com/science/article/abs/pii/S0032591014008158

[136] “[PDF] Au@TiO2 nanocomposites for the catalytic degradation of methyl orange and methylene blue: An electron relay effect | Semantic Scholar.” Accessed: Jun. 13, 2024. [Online]. Available: https://www.semanticscholar.org/paper/Au%40TiO2-nanocomposites-for-the-catalytic-of-methyl-Khan-Lee/4de1b99c51989b48feb3d4a57fa9cc147370d9b2

[137] “Catalytic Reduction of Methylene Blue Dye by Copper Oxide Nanoparticles | Journal of Cluster Science.” Accessed: Jun. 13, 2024. [Online]. Available: https://link.springer.com/article/10.1007/s10876-020-01950-0

[138] “One pot preparation of CeO2@Alginate composite beads for the catalytic reduction of MB dye: Effect of cerium percentage | Semantic Scholar.” Accessed: Jun. 13, 2024. [Online]. Available: https://www.semanticscholar.org/paper/One-pot-preparation-of-

CeO2%40Alginate-composite-for-Benali-Boukoussa/966943b0be39399afe6a337bd0aea5055692fdd9

[139] B. N. E. Houda and A. Madjda, "Préparation de nanoparticules métalliques supportées sur une argile : Applications au traitement des eaux usées," Master's thesis, Université des Sciences et de la Technologie d'Oran « Mohamed BOUDIAF », Faculté de Chimie - Département de Génie des Matériaux, 2023.